



Review

Multicomponent halide templating: The effect of structure-directing agents on the assembly of molecular and extended coordination compounds

Colm Healy ^{*}, Wolfgang Schmitt ^{*}

School of Chemistry & CRANN, University of Dublin, Trinity College, Dublin 2, Ireland



ARTICLE INFO

Article history:

Received 9 April 2018

Received in revised form 11 May 2018

Accepted 14 May 2018

Keywords:

Multicomponent synthesis
Template
Anion
Coordination compounds
Structure
Supramolecular chemistry

ABSTRACT

This account covers template effects that lead to the formation of polynuclear coordination compounds, with a focus on how the interplay of the structure-directing effects of multiple agents (including inorganic anions and organic ligands) combine to influence the geometry and nuclearity of metal-containing assemblies. Simple anions and ligands impart defined geometric shapes (triangles, squares, hexagons) onto oligonuclear assemblies, and these shapes can combine to produce a range of more sophisticated metallo-supramolecular architectures (including Platonic and Archimedean solids). An understanding of the structure-directing effects of simple templates is therefore necessary to predict or rationalise such polynuclear architectures, which may have wide-ranging applications in catalysis, in magnetism, as sensors, etc. This article primarily focuses on halide-templated assemblies of first row transition metal ions (particularly manganese coordination clusters and vanadates), but the principles discussed herein are applicable to a much wider range of coordination compounds.

© 2018 Elsevier B.V. All rights reserved.

Contents

1. Introduction	68
2. Polynuclear coordination compounds	68
3. Structure-directing μ_3 -halide ions	70
3.1. Halide-centred {M ₃ X} triangles	70
3.2. Halide-capped {M ₃ X} triangles	71
3.2.1. Supertetrahedra	71
4. Structure-directing μ_4 -halide ions	72
4.1. Halide-centred {M ₄ X} squares	72
4.2. Halide-capped {M ₄ X} squares	72
4.2.1. Shuttlecocks	72
4.2.2. Cuboctahedra	74
4.2.3. Vanadates	75
5. Structure-directing μ_5 -halide ions	77
6. Structure-directing μ_6 -halide ions	79
7. Larger entities	80
8. Conclusions	81
Declaration of interest	82
Acknowledgements	82
Appendix A. Supplementary data	82
References	82

* Corresponding authors.

E-mail addresses: healyc6@tcd.ie (C. Healy), schmittw@tcd.ie (W. Schmitt).

1. Introduction

All synthetic supramolecular, self-assembly or coordination chemistry approaches rely, on some level, on template effects or related structure-directing effects, whereby the geometry and nuclearity of the final product depends on the preferred geometries of the starting materials. In simple situations, the structure-directing effects are trivial to predict and understand, but in order to generate more sophisticated supramolecular structures, multiple templating effects must be taken into account. In many cases, several distinct classes of reactants (metal ions, inorganic counterions, organic ligands) must work in concert with one another to generate a desired structure.

The interplay of multiple distinct components during self-assembly reactions has been recognised for some time. Lehn et al. demonstrated in 1997 that a combination of anion and ligand structure-directing effects controlled the nuclearity of the circular helicate molecules, generating tetranuclear, pentanuclear or hexanuclear examples of iron helicates [1]. These principles were recently elaborated upon by Leigh et al. to generate sophisticated interlocked knot systems including the 8_{19} knot and pentafoil knots (Fig. 1) [2–4]. Supramolecular cage structures are also well known to depend on both supporting ligand and central anion template effects to determine cage sizes and geometries [5–7]. Similarly, topology and pore size in metal–organic framework (MOF) structures can be controlled using combinations of structure-directing effects involving multiple components [8–11].

Clearly, many diverse and interesting structures of metal-containing assemblies can be generated by careful control (or serendipitous application) of anion and ligand effects. In this account, we aim to emphasise the combination of structure-directing effects from multiple anionic components, and how these effects combine to influence the geometry, nuclearity, and properties of selected, polynuclear coordination compounds. The interactions which hold these diverse structures together range from weak electrostatic and van der Waals forces to strong, quasicovalent interactions. Much attention has previously been given in the literature to electrostatic and hydrogen bonding effects when examining supramolecular assemblies [12–15]. For details of anion-ligand interactions and self-assembly processes, the reader is directed towards recent review articles by Beer et al. [16–19]. Here, we focus on systems where coordination bonds are the primary structure-directing mechanism. A comprehensive review of such a vast area of synthetic chemistry is, of course, simply impractical – therefore, in this account we will restrict the focus to selected systems containing first-row transition metals, where at least one structure-directing agent in the system is a halide. This restriction is somewhat arbitrary, but the highlighted synthetic concepts are generally applicable to a wide array of coordination compounds. For conceptual clarity, the compounds dis-

cussed in this review will be grouped by the connectivity of halide ions, emphasising their structure-directing effects as nucleophiles and donor ligands.

2. Polynuclear coordination compounds

Coordination complexes with terminal metal–halide (M–X) bonds are well known. In these systems, the halide ions act as simple, monodentate ligands to single metal centres, and thus do not impart significant structure-directing effects. However, structural diversity increases somewhat as one extends towards bridging halide donors, which can generate complex polynuclear coordination compounds.

Polynuclear metal assemblies (*i.e.* coordination compounds containing multiple metal centres in reasonably close electronic contact with one another) are an important class of coordination compound. The combination of multiple metal centres in close proximity gives rise to interesting electronic and magnetic properties. Much attention has been devoted over the past decades to the study of magnetic interactions in these compounds, with the interactions between paramagnetic metal centres in close proximity to one another giving rise to complex ferromagnetic or antiferromagnetic behaviours, uncompensated magnetic moments, slow relaxation of the magnetic moment and quantum effects [20,21]. In particular, the subclass of single molecule magnets (SMMs) have attracted particular attention in recent years, and have been postulated as potential components in high-density data storage devices [20,22].

Polynuclear coordination compounds also find use in catalytic studies, as multiple charge equivalents can be accumulated on a single molecule across several redox-active metal sites. This can be useful in catalysing multiple-electron reactions, for example the four-electron water oxidation reaction [23–26]. The well-defined molecular environments allow an insight into the details of catalytic reactions and how perturbations of the catalytic geometry affect the reactivity.

Synthetically, the formation of these compounds is often governed by template effects. Coulombic repulsion between positively charged metal centres must be overcome in order to generate polynuclear entities [27]. This can be achieved using organic ligand or inorganic anion stabilisation effects, or a combination of the two. When rationalising the overall geometry of a polynuclear coordination compound, therefore, it can be sensible to describe the structure by the geometry imparted by the stabilising or structure-directing agents (Fig. 2).

Simple stabilising agents have a preferred geometry, and will tend to bias a reaction system towards a specific geometry. However, most stabilising agents have multiple possible coordination geometries – this is demonstrated in the case of phosphonate ligands in Fig. 2a [28]. These preferred geometries can be repre-

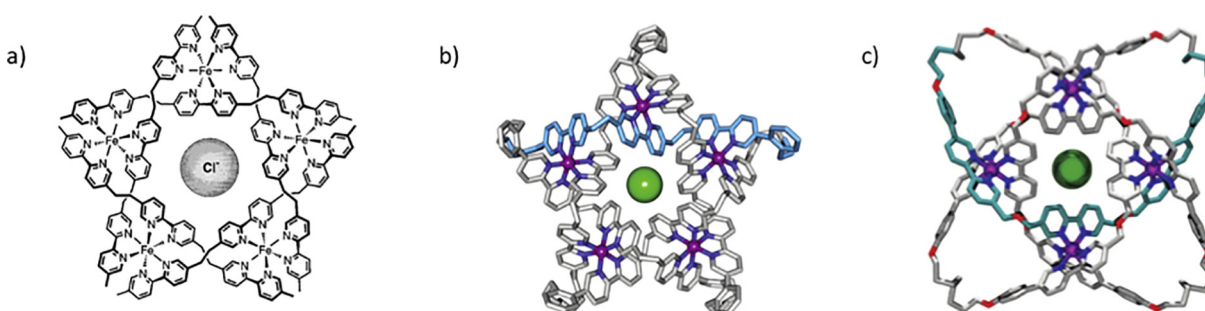


Fig. 1. Many of the most impressive supramolecular assemblies require combinations of multiple structure-directing agents (metals, ligands and anions) in order to form, including a) the iron helicates by Lehn et al. b) the pentafoil knot by Leigh et al. c) the 8_{19} knot by Leigh et al. [1,2,4]. Reproduced with permission of ACS and Science (AAAS).

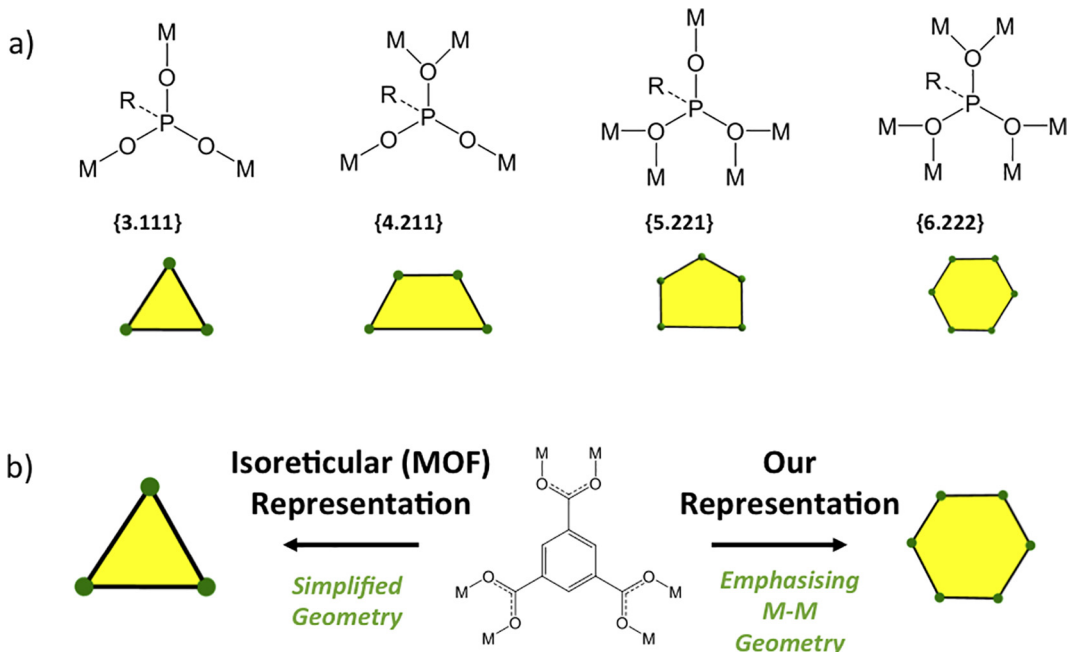


Fig. 2. a) Some binding modes of phosphonate ligands (as an example), along with the Harris notation [28] and geometrical representations of the binding mode. b) In order to emphasise the structure-directing effects of ligands on metals, we define ligand geometry in this article by the geometry of the metal centres.

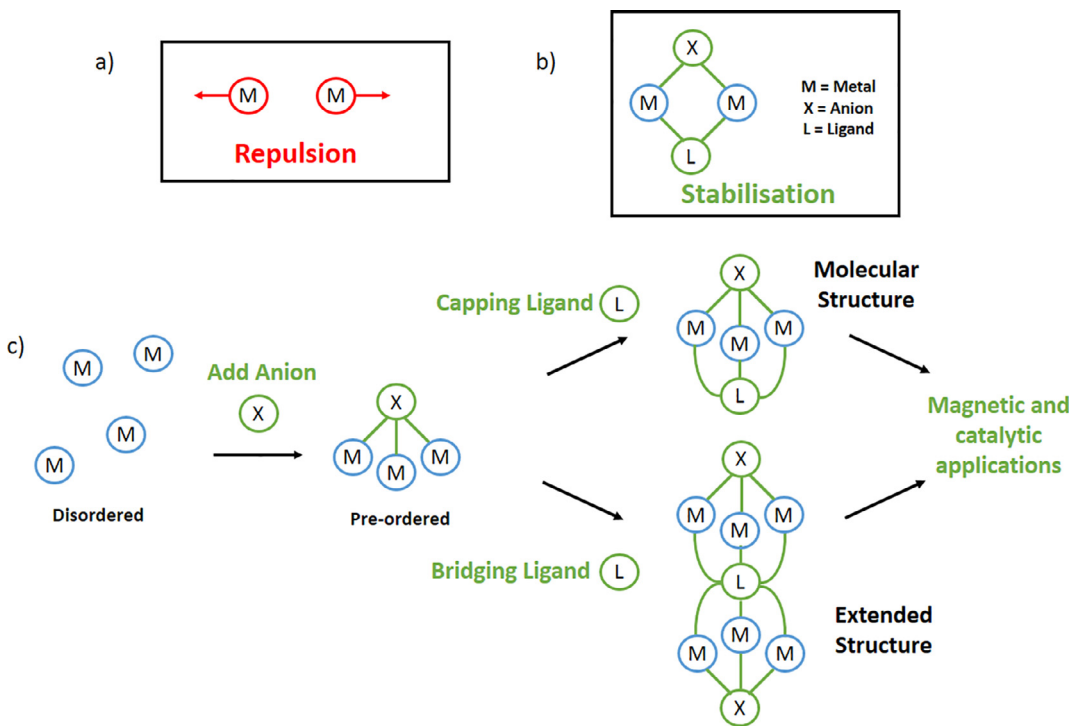


Fig. 3. a) Coulombic repulsion between metal centres in solution prevents the aggregation of polynuclear metal assemblies. b) Interactions between metals and structure-directing agents (anions and ligands) can overcome Coulombic repulsion to stabilise polynuclear assemblies. c) Interactions between metals and structure-directing anions can generate transient polynuclear assemblies with well-defined geometries. If a suitable structure-directing (anionic or neutral) ligand is present, these pre-ordered assemblies can be trapped into either molecular or extended materials.

sented as simple two-dimensional geometric shapes. While the binding mode of a given structure-directing agent can sometimes be difficult to predict from first principles, this approach allows structures to be understood in simple terms.

Given that multiple geometries can be achieved by simple stabilising agents, it is rational to consider multiple structure-

directing agents in conjunction with one another (Fig. 3). In the case of simple metal halide solutions, the halide ions can engage in multiple (possibly weak) coordination bonds to several metal centres, compensating for repulsion between the positively charged ions. This will tend to happen in a transient manner, with multiple possible conformations of halide-templated assemblies

existing in equilibrium with one another. A second structure directing agent (ligand) which prefers one of the transient geometries over the others can effectively “trap” the system into a specific geometry. Thus, it is the combination of multiple structure-directing agents, which determines the final product. Strategic choice of structure-directing agents can generate either molecular or extended structures with the targeted physicochemical properties (Fig. 3).

3. Structure-directing μ_3 -halide ions

3.1. Halide-centred $\{M_3X\}$ triangles

One of the simplest halide-templated geometry for metal centres to adopt is the halide-centred $\{M_3X\}$ triangle, where the structure-directing halide (X) ion coordinates to three metal centres in a μ_3 binding mode. Triangular metal assemblies are particularly interesting in the context of paramagnetic metal ions, as the three metal centres cannot achieve an antiferromagnetic spin-pairing arrangement, thus giving rise to uncompensated spin states and resulting in a non-zero spin ground state [29–31]. However, the halide-centred arrangement is quite uncommon for first row transition metals, requiring cooperation from relatively specific ligands to stabilise the arrangement.

One approach towards stabilising $\{M_3X\}$ motifs is to generate cage-like “cyclophane” ligands (Fig. 4a) [32–34]. These ligands effectively force a triangular metal arrangement, which requires a central ion to satisfy the bonding requirements of the three metal ions. Murray et al. have generated examples with iron (II), manganese (II) and cobalt (II) triangles stabilised by central chloride or bromide ions [32–34]. However, size constraints result in significant distortion in these cage systems, with combinations of terminal and bridging halides required to satisfy coordination

environments [33]. The bromide analogues are sufficiently distorted that the stabilising bromides may be displaced (for example by bridging hydride ligands, which can subsequently be used for CO_2 reduction) [32,34].

In comparison, Helicates offer a more flexible platform for generating $\{M_3X\}$ triangles [35–37]. Polydentate N-donor ligands have been demonstrated to be able to accommodate $\{M_3X\}$ motifs of varying sizes, with the smaller $\{M_3O\}$ triangle inducing an $\{M_5O\}$ “mesocate” structure while the larger $\{M_3Cl\}$, $\{M_3Br\}$ or $\{M_3I\}$ triangles induce larger $\{M_8X_2\}$ helicate structures [38]. The $\{M_8X_2\}$ helicates contain two $\{M_3X\}$ triangular motifs stabilised by three capping N-donor ligands in a screwed arrangement. Anion substitution can switch the system between $\{\text{Mn}_5\text{O}\}$ and $\{\text{Mn}_8\text{Cl}_2\}$ arrangements [37].

While $\{M_3X\}$ -centred triangles are relatively rare for the first row metals, a general exception to this rule seems to be the $\{\text{Co}_3\text{F}\}$ triangle. Winpenny et al. reported numerous examples of polynuclear cobalt entities stabilised by phosphonate and carboxylate ligands, several of which contained $\{\text{Co}_3\text{F}\}$ triangle units [39–41]. $\{\text{Co}_3\text{F}\}$ triangles have also been reported as components in extended solids [42–44]. A particularly exciting example of a structure with $\{\text{Co}_3\text{F}\}$ triangles is a remarkable $\{\text{Co}_{12}\}$ coordination cluster, $[\text{Co}_{12}\text{F}_4(\text{PO}_4)_4(\text{H}_2\text{O})_6]^{8+}$ [45]. In this structure, the twelve cobalt ions define the vertices of a truncated tetrahedron (an Archimedean solid generated from four triangular and four hexagonal faces). Each triangular face is represented by a $\{\text{Co}_3\text{F}\}$ unit, while each hexagonal face is represented by a $\{\text{Co}_6(\text{PO}_4)\}$ unit, with the phosphate coordinating in a {6.222} mode [45]. In a principle that will be demonstrated repeatedly throughout this review, the structure-directing effects of two distinct components (fluoride and phosphonate) are required to generate this particular geometry.

The edge of each triangular face in the $\{\text{Co}_{12}\}$ unit is capped by a carboxylate ligand. In the example presented, bridging ferrocene-type ligands are used to bridge between the $\{\text{Co}_{12}\}$ units, generat-

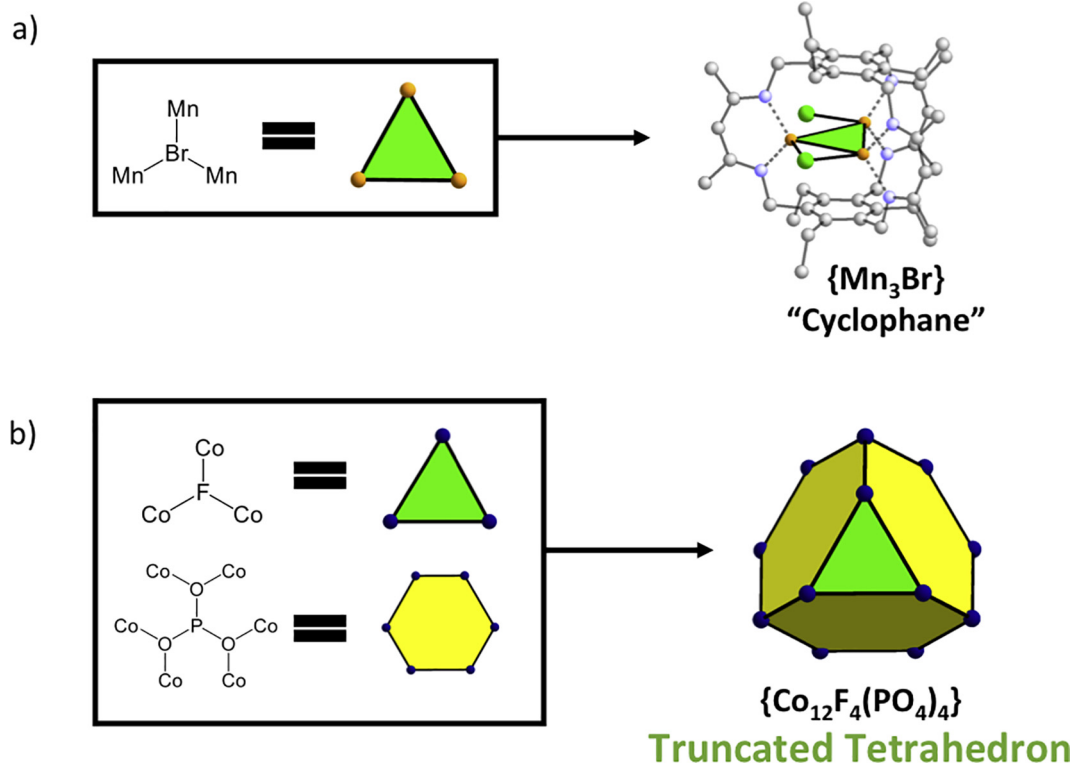


Fig. 4. a) The simple halide-centred $\{M_3X\}$ motif can be stabilised by “cyclophane” cage ligands. b) The $\{\text{Co}_{12}\}$ unit with the geometry of a truncated tetrahedron can be assembled from four triangular $\{\text{Co}_3\text{F}\}$ faces and four $\{\text{Co}_6(\text{PO}_4)\}$ faces [33,35].

ing an impressive extended framework structure [45]. The framework was investigated for its gas sorption properties, and the authors note the potential utility of the truncated octahedron node as a building unit in MOF chemistry. One potential drawback of the unit is that formation seems to be sensitive to reaction conditions – the authors note that *in situ* hydrolysis of PF_6^- is required to generate the fluoride, and speculate that a bulky, zwitterionic linker might be necessary for framework formation [45]. Nevertheless, this structure is quite remarkable and may find interesting uses in future.

3.2. Halide-capped $\{\text{M}_3\text{X}\}$ triangles

In contrast to halide-centred triangles, halide-capped triangles are extremely common. In this arrangement, the halide ion is displaced from the centre of the metal ions and is instead located above the plane of metal ions. Numerous examples of this motif are reported in the literature, using a variety of metal ions and capping halides, of which only some are cited here [46–52]. The prominence of this structural motif in the literature highlights a strong preference for this geometry and indicates a significant structure-directing effect on behalf of the halide ion. In many examples, the triangular unit only requires terminal ligands (commonly ethylenediamine or related capping ligands) to stabilise the structure [48–52]. Helicates similar to those discussed above are also known – in some examples multiple triangles within a helix structure will share capping halide ions [53,54].

The halide-capped triangle is particularly prominent in cubane-type systems [55–60]. These structures can be considered as being composed of four metal centres that adopt a tetrahedral arrangement, with each triangular face capped by a $\mu_3\text{-X}$ ligand (the metal ions and capping ligands combined then define the vertices of a cube). This can be achieved in an $\{\text{M}_4\text{X}_4\}$ fashion [55–57], or in a $\{\text{M}_4\text{O}_3\text{X}\}$ fashion [58–60]. In the late 80s and early 90s, $\{\text{M}_4\text{O}_3\text{X}\}$ systems were heavily investigated in an attempt to elucidate the structure and reactivity of the active centre of photosystem II (PSII), a key component in photosynthesis [61–66]. Cubane units can also be used as building units in larger structures [67]. A related $\{\text{M}_4\text{X}_6\}$ structure is sometimes described as a “double cubane” – this can be conceptualised as two face-sharing cube units, with two opposing metal centres removed [68].

3.2.1. Supertetrahedra

As demonstrated by the $\{\text{Co}_{12}\}$ truncated tetrahedron described above, the combination of multiple structure-directing motifs onto a single molecule allows complicated geometries (including Platonic and Archimedean solids) to be accessed. Further modification of the templating units can introduce further structural sophistication and complexity. This principle is demonstrated by the family of manganese compounds, the $\{\text{Mn}_{10}\}$ supertetrahedra (Fig. 5).

The core of the $\{\text{Mn}_{10}\}$ supertetrahedron can be considered as a $\{\text{Mn}_6\}$ octahedron. As a simple platonic solid, an octahedron can be generated by a combination of eight simple triangular faces. Since both μ_3 -halides and μ_3 -oxo ligands generate triangular geometries, $\{\text{Mn}_6\}$ octahedra can be generated from alternating $\{\text{Mn}_3\text{X}\}$ and

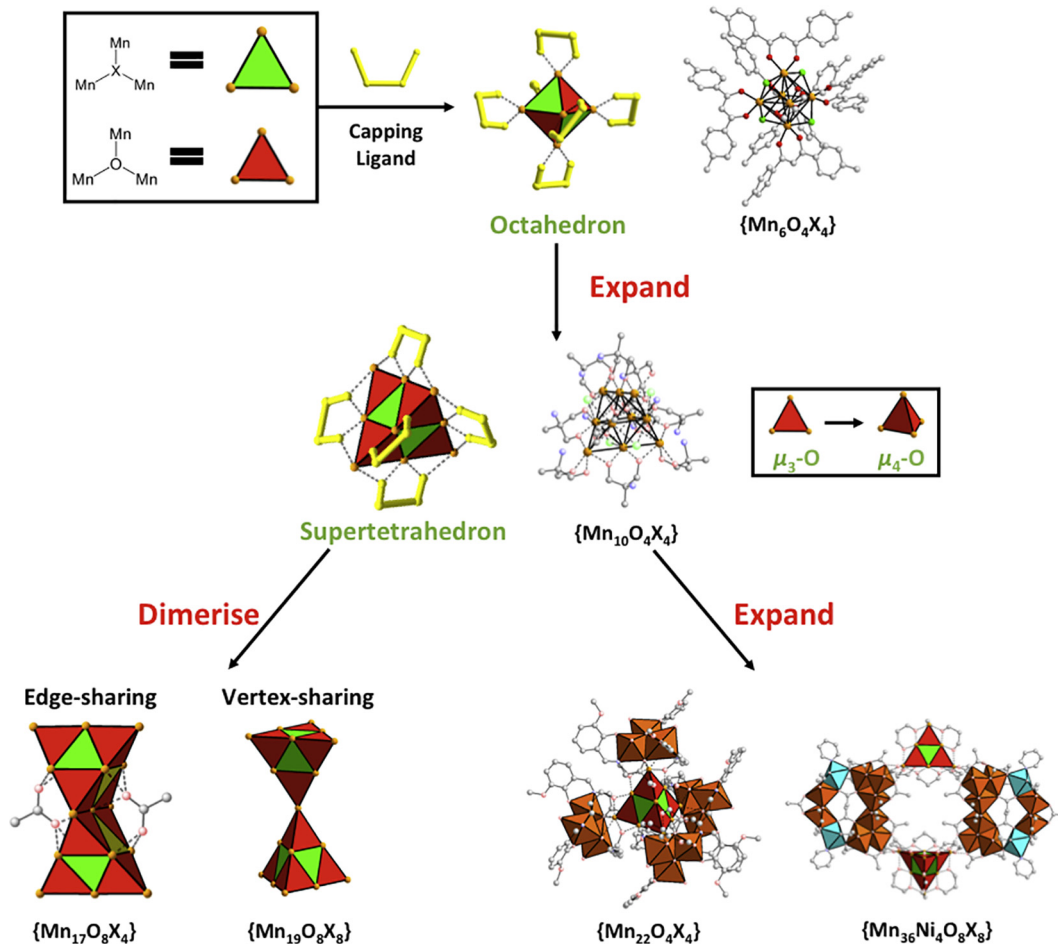


Fig. 5. Octahedral $\{\text{Mn}_6\}$ motifs can be generated using combinations of $\{\text{Mn}_3\text{X}\}$ and $\{\text{Mn}_3\text{O}\}$ triangles. Expansion of the $\{\text{Mn}_3\text{O}\}$ triangle to an $\{\text{Mn}_4\text{O}\}$ tetrahedron can generate an $\{\text{Mn}_{10}\}$ “supertetrahedron”. The supertetrahedron can be further assembled into $\{\text{Mn}_{17}\}$, $\{\text{Mn}_{19}\}$, $\{\text{Mn}_{22}\}$ and $\{\text{Mn}_{36}\text{Ni}_4\}$ units [81,82,89,90].

$\{Mn_3O\}$ triangles, in the presence of suitable capping ligands. This strategy has been exploited to isolate $\{Mn_6O_4Cl_4\}$ and $\{Mn_6O_6Br_2\}$ compounds. Reports on these compounds have focused on their magnetic properties [69–71].

The $\{Mn_6O_4X_4\}$ octahedral motif can be conceptually expanded to generate the supertetrahedron. By expanding the $\{Mn_3O\}$ triangles to $\{Mn_4O\}$ tetrahedra, an additional four Mn centres can be incorporated onto the octahedral core. These four centres define the supertetrahedron (Fig. 5). These species have been isolated with a range of μ_3 -halide (Cl^- , Br^- , I^-) or μ_3 -pseudohalide (N_3^-) structure-directing agents [72–78]. Capping ligands bridge between the metal centres along the edges of the supertetrahedron, with several binding motifs possible. $\{Mn_{10}\}$ supertetrahedra are generally mixed-valence species, but careful manipulation of the capping ligands can force a redistribution of the Mn^{II} and Mn^{III} centres within the structure [79]. A related $\{Mn_9\}$ structure can also be generated using similar building principles [80].

In addition to showcasing geometric building principles rather well, the $\{Mn_{10}\}$ supertetrahedron units are particularly interesting when considered as building units in larger structures. Several remarkable species have been generated using the $\{Mn_{10}\}$ unit as a subcomponent, constructed from the same building principles as described above [81–88]. Dimers of the $\{Mn_{10}\}$ building unit have been reported by Powell et al. The unit can be dimerised in either a vertex-sharing or edge-sharing manner. The edge-sharing $\{Mn_{17}\}$ analogues make use of carboxylate ligands in {5.32} binding modes to bridge between the two supertetrahedral units [75,89]. Meanwhile, the vertex-sharing $\{Mn_{19}\}$ analogue is particularly interesting in the context of molecular magnetism. Ferromagnetic interactions between the metal centres impart a $S = 83/2$ spin ground state to the molecule, the maximum possible for a $\{Mn_{12}^{III}-Mn^{II}\}$ system [81]. This molecule held the record for the highest spin value for nearly a decade before being surpassed by an $\{Fe_{42}\}$ compound [90]. The magnetic interactions between the spin centres in $\{Mn_{19}\}$ are mediated predominantly by the μ_4 -oxo ligands, and so the spin state is insensitive to substitution of the templating species (N_3^- , Cl^- , Br^- , ^-OMe have all been used) [82,83].

Moreover, the central ion at the shared vertex of the $\{Mn_{19}\}$ molecule can be replaced by a variety of ions to generate $\{Mn_{18}M\}$ species [84,85]. Diamagnetic M species at this position effectively separate the two supertetrahedral subunits, with varying degrees of magnetic interactions between the two subunits depending on the nature of the central ion [84]. Introducing anisotropic ions such as Dy^{III} into this position was also shown to be an effective method of significantly increasing the anisotropy of the system, generating single molecule magnet (SMM) behaviour [85]. The capping ligands on $\{Mn_{19}\}$ species can also be substituted – this has very little impact on the magnetic interactions, but does generate interesting building units which could potentially be functionalised further [86].

By using bridging ligands, the $\{Mn_{10}\}$ supertetrahedron can be further connected to other metal centres to generate larger entities. In one such example, chiral Schiff base ligands were used to connect the $\{Mn_{10}\}$ supertetrahedron to four $\{Mn_3\}$ units, generating an impressive $\{Mn_{22}\}$ structure with 12 stereogenic centres [87]. The structure can be considered as composed of four $\{Mn_4\}$ tetrahedra, each sharing a vertex with a central $\{Mn_{10}\}$ supertetrahedron. The compound displays both ferroelectric and ferromagnetic properties [87].

A truly remarkable structure generated using supertetrahedral building units is the mixed metal $\{Mn_{36}Ni_4\}$ system. This consists of two $\{Mn_{10}Cl_4\}$ supertetrahedra, which are connected via bridging acetate ligands to two $\{Mn_8Ni_2\}$ “loop” units [88]. The system is noteworthy for the simplicity of the building units which generate the structure – in addition to the Cl^- and O-donor templates required for the $\{Mn_{10}\}$ subunits, the entire system is supported

only by propanediol, acetate and pyridine ligands [88]. This system is a nice example of how intricate, well-defined architectures can be generated from simple templating or structure directing units.

4. Structure-directing μ_4 -halide ions

4.1. Halide-centred $\{M_4X\}$ squares

Moving to $\{M_4X\}$ structural units, Hirotsu et al. provides a neat demonstration of the complementarity of ligand and anionic template in generating different $\{M_4\}$ structures [91]. By using the same xanthene-derived polydentate O- and N-donor ligand but changing the anionic template, both the connectivity and the oxidation state of the resulting $\{Mn_4\}$ compound could be manipulated [91]. Acetate anions afforded a mixed-valent, oxo-bridged “double cubane” structure, while chloride anions afforded a chloride-centred, all-manganese (III) square structure (Fig. 6a) [91]. This structure has a simple $\{M_4X\}$ motif where the halide is located at the centroid of a square unit composed of $Mn^{(III)}$ ions.

This simple $\{M_4X\}$ square motif can be isolated as a molecular structure in the case of cobalt (II) using bulky, stabilising pyrazolate-type ligands with two chelating N-donor sites that complement the geometry of the square template [92]. The same ligand motif can be used to generate bromide-centred nickel (II) squares (Fig. 6b) [93]. More commonly, this halide-centred $\{M_4X\}$ square motif is found in extended structures, rather than discrete complexes (Fig. 6b). Various ligands can bind across the edge of the $\{M_4X\}$ square, usually with two ligands capping each M-M edge to generate an eight-coordinate $\{M_4L_8X\}$ node. Using reticular synthesis concepts [94], this eight-coordinate node can be connected into extended, porous framework structures using linear or triangular linker ligands.

Numerous examples of these frameworks have been prepared, using first row transition metals (Mn, Fe, Co, Cu, Ni and Zn) with bridging linker ligands (carboxylate, pyrazolate, triazolate and tetrazolate) of various geometries [95–109]. As is common for framework compounds, applications focus principally on host-guest interactions such as gas capture/storage/separation [95–99], with a slightly lesser focus on catalysis [100] and magnetism [101,102]. The formation of this node has been shown to be sensitive to substitution of solvent [102] or counterion [103].

In some cases, direct synthesis of this node is not possible. However, transmetalation has been shown to be a successful avenue towards frameworks with this $\{M_4X\}$ square motif in the nodes, including in a single-crystal-to-single-crystal fashion [104,105]. In one example, a manganese (II) tetrazolate MOF with crystallographically distinct metal sites (*intra-* and *extra-framework*) was transmetalated with iron (II), copper (II) or zinc (II) [106]. Using a multiwavelength anomalous dispersion (MAD) X-ray technique, the extent of substitution, as well as the crystallographic position of the substituting ions in this framework, could be quantified [106].

The $\{M_4X\}$ square motif can also be stabilised by calixarene-type ligands. Calix[4]arene ligands possess four O-donor ligands in a suitable geometry to stabilise the square structure, if the square is sufficiently small. Fluoride-centred manganese (II) square motifs supported by two calix[4]arenes have been reported, where two macrocyclic ligands cap each side of the square. The structures were investigated for photophysical and magnetic properties [110,111].

4.2. Halide-capped $\{M_4X\}$ squares

4.2.1. Shuttlecocks

Whilst calix[4]arenes can be applied to stabilise the above described complexes, calixarene-type ligands are more commonly

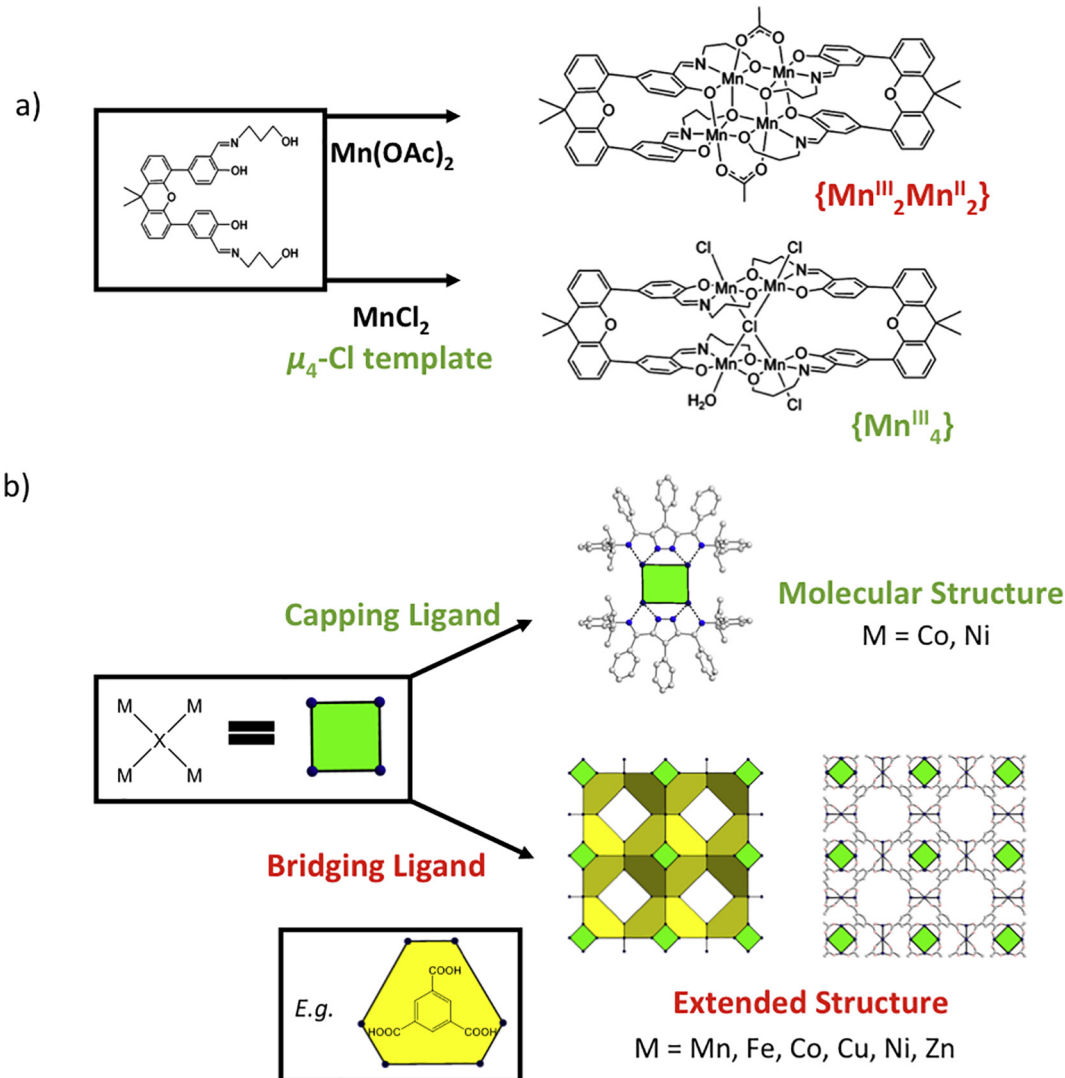


Fig. 6. a) The importance of halide template effects is demonstrated for a xanthene-derived polydentate ligand, which forms $\{\text{Mn}^{\text{III}}_2\text{Mn}^{\text{II}}_2\}$ structures when combined with manganese acetate, but $\{\text{Mn}^{\text{III}}_4\}$ structures in the presence of a $\mu_4\text{-Cl}^-$ chloride template. b) The $\{\text{M}_4\text{X}\}$ square motif (featuring a $\mu_4\text{-X}$ template) can be combined with either capping or bridging ligands to generate molecular or extended structures [91,92,108].

used in conjunction with halide templates to generate “shuttlecock”-structured assemblies. These compounds exploit the $\{\text{M}_4\text{X}\}$ capped square motif, where the templating halide ion caps the plane of a $\{\text{M}_4\}$ square (Fig. 7a). This geometry is suitable for thiocalix[4]arenes to bind to the face opposite the halide. The complementary concave geometries of both the $\{\text{M}_4\text{X}\}$ capped square motif and the thiocalix[4]arene ligands generates concave assemblies with hydrophobic binding pockets.

Although some examples have been generated using iron (II) and nickel (II) [112,113], the most common examples of this motif are chloride-capped cobalt (II) $\{\text{Co}_4\text{Cl}\}$ shuttlecock structures. This structure possesses peripheral binding sites, which are commonly occupied by carboxylate ligands. Neatly, these carboxylate ligands can be displaced by polytopic carboxylate ligands, connecting several shuttlecock units into larger structures (Fig. 7b). For example, in 2012 Liu et al. used tritopic carboxylate ligands to generate a $6 \times \{\text{Co}_4\text{Cl}\}$ nanocage structure. When only the metal atoms are considered, this structure has a truncated octahedron core, with the concave calixarene entities capping each square face of the structure [114]. By varying the size of both the linking carboxylates and the calixarene capping ligands, either of the two potential

binding pockets in this molecule (the cage core or the calixarene pocket) could be modified (Fig. 6b) [114].

Various linking units have been used to generate connected structures from this motif. The multiple binding modes of phosphonate ligands can be used to connect these $\{\text{Co}_4\text{Cl}\}$ shuttlecocks into dimers, trimers or tetramers [115]. Cage, grid and polymer aggregates are also possible using linking carboxylate or pyridyl ligands, depending on reaction conditions [116–119]. In one example, bifunctional pyridine-carboxylate linkers were used to switch between $4x\{\text{Co}_4\text{Cl}\}$ tetrahedra and $4x\{\text{Co}_4\text{Cl}\}$ cylinders by manipulating linker coordination modes via altering pH conditions [120]. Probably the most interesting connector units are $\{\text{MoO}_4\}$ or $\{\text{WO}_4\}$ units, which were used to generate an octahedral $6 \times \{\text{Co}_4\text{Cl}\}$ shuttlecock structure [121]. These metallosupramolecular species are analogous in structure to the nanocage presented in Fig. 7b, and represent the first examples of mixed-metal assemblies derived from the $\{\text{Co}_4\text{Cl}\}$ shuttlecock structure. Further studies on shuttlecock structures have largely focused on host-guest interactions or magnetic behaviour.

While the formation of the shuttlecock structure is possible without chloride influence [122], the combination of thiocalix[4]

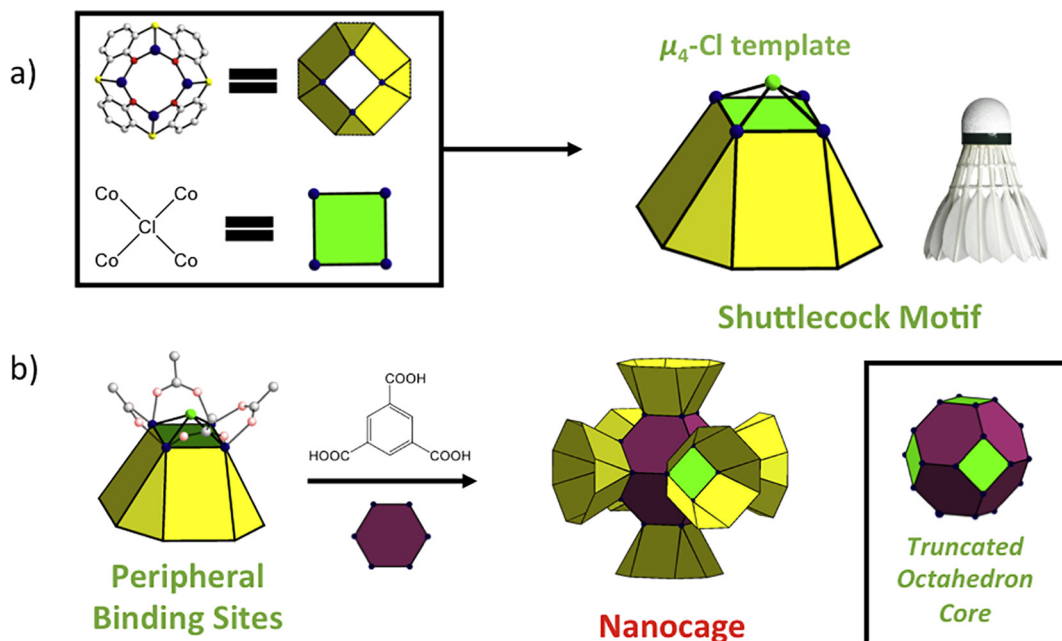


Fig. 7. a) The combination of the concave $\{M_4X\}$ “capped square” motif with complimentary concave thiacalix[4]arene ligands can generate shuttlecock structures. b) The metal centres in the shuttlecock motif retain peripheral binding sites, which allow individual shuttlecock entities to be further self-assembled into larger architectures including polymers and cages. The example shown here is a $6\times\{\text{Co}_4\text{Cl}\}$ nanocage with a truncated octahedron core [114].

arene ligands with first row transition metal ions in the absence of halides does not guarantee the formation of the shuttlecock structure [123,124], indicating that halide and ligand are acting in a cooperative fashion to generate the shuttlecock structure. The most common approach to displace the chloride ion from these structures is by oxidising the sulfur units to sulfonyl units, generating additional stabilising O-donor atoms on the ligand [119]. In this configuration the role of the capping halide ion can be replaced by an oxo-ligand [125–128]. These shuttlecock assemblies have some potentially very interesting uses in catalysis [129].

4.2.2. Cubooctahedra

Archimedean solids are a set of fundamental three-dimensional shapes generated from combinations of regular polygons. In principle metallosuramolecular synthesis concepts allow these shapes to be rationally generated by imparting the combination of multiple structure-directing motifs during the formation of a targeted molecule.

This synthetic principle is demonstrated by a family of manganese (III) phosphonates (Fig. 8) [130,131]. The parent structure for this family, $[\text{Mn}_{13}\text{O}_8\text{Cl}_6(\text{tert-butyl-PO}_3)_8]$, possesses the geometry of a cuboctahedron (an Archimedean solid generated from six square and eight triangular faces). In this highly symmetric structure, the eight phosphonate ligands cap each of the triangular faces in a {3.111} binding mode (representing the points of a cube), while the six chloride ions cap each square face (representing the points of an octahedron) [130]. In combination with a $\{\text{Mn}^{\text{II}}\text{O}_8\}$ cubic core, the separate square and triangular structure-directing effects combine to stabilise the $\{\text{Mn}_{13}\}$ geometry. All of the Jahn-Teller elongated axes of the manganese (III) centres align in the direction of the chloride capping units, indicating a preference for μ_4 -chloride ligands to locate in kinetically labile Jahn-Teller sites [130].

Perturbation of this parent cluster allows access to different (generally lower symmetry) analogues of the $\{\text{Mn}_{13}\}$ structure, with the geometry and nuclearity of the resulting species determined by the templating species which bind to the cluster. One

such structure is a $\{\text{Mn}_{12}\}$ analogue $\text{H}_5[\text{Mn}_{12}\text{O}_8\text{Cl}_4(\text{tert-butyl-PO}_3)_{10}]^{2-}$, which is conceptually related to the parent $\{\text{Mn}_{13}\}$ structure by removing two adjacent chloride units and the manganese centre between them, effectively leaving a vacancy or lacuna in the structure (Fig. 8) [131]. Two additional phosphonate ligands are recruited and some rearrangement of the phosphonate binding modes around the lacunary site occurs to stabilise the compound [131].

A series of analogous structures can be obtained by the formal insertion of one, two or three manganese centres into this lacunary site, stabilised by the dangling phosphonate ligands around the lacuna site. A lower-symmetry $\{\text{Mn}_{13}\}$ structure, $\text{H}_5[\text{Mn}_{13}\text{O}_9\text{Cl}_5(\text{tert-butyl-PO}_3)_{10}]^{2-}$, can be formally constructed by the insertion of an additional manganese (III) centre into the lacunary $\{\text{Mn}_{12}\}$ structure. The additional manganese centre is capped by a monodentate chloride ligand. Similarly, a $\{\text{Mn}^{\text{II}}\text{-OH-Mn}^{\text{III}}\}$ unit, along with an additional peripheral phosphonate ligand, can bind into the lacunary site to generate a chiral $\{\text{Mn}_{14}\}$ structure, $\text{H}_2[\text{Mn}_{14}\text{O}_9\text{Cl}_4(\text{tert-butyl-PO}_3)_{11}(\text{aminopyridine})]^{2-}$. Finally, a $\{\text{Mn}^{\text{II}}\text{Mn}^{\text{III}}\text{O}\}$ unit can be incorporated into the lacunary site to generate a $\{\text{Mn}_{15}\}$ structure. These influence of nuclearity and asymmetry of these compounds on their magnetic properties was investigated [130,131].

When the relative chloride content of the cluster is further reduced an interesting $\{\text{Mn}_{15}\}$ structure, $\text{H}_4[\text{Mn}_{15}\text{O}_8\text{Cl}_2(\text{tert-butyl-PO}_3)_{12}(\text{MeO})_6]^{2-}$, can be isolated [131]. Conceptually, this can be understood by taking the symmetric $\{\text{Mn}_{13}\}$ parent compound, generating two lacunary sites on opposite sides of the structure, and introducing $\{\text{Mn}^{\text{II}}\text{-OH-Mn}^{\text{III}}\}$ units into both of these lacunae. The symmetry of the parent compound is significantly distorted in this analogue, giving rise to significant magnetic anisotropy due to the rearrangement of the Jahn-Teller axes of individual Mn^{III} centres [131]. In this case the anisotropy in the structure is sufficient to result in slow relaxation of the magnetisation and single molecule magnet (SMM) behaviour [131].

When no structure-directing halide ions bind to the cluster, a final example of the $\{\text{Mn}_{13}\}$ family, $\text{H}_4[\text{Mn}_{13}\text{O}_8(\text{tert-butyl-PO}_3)_{12}]^{2-}$

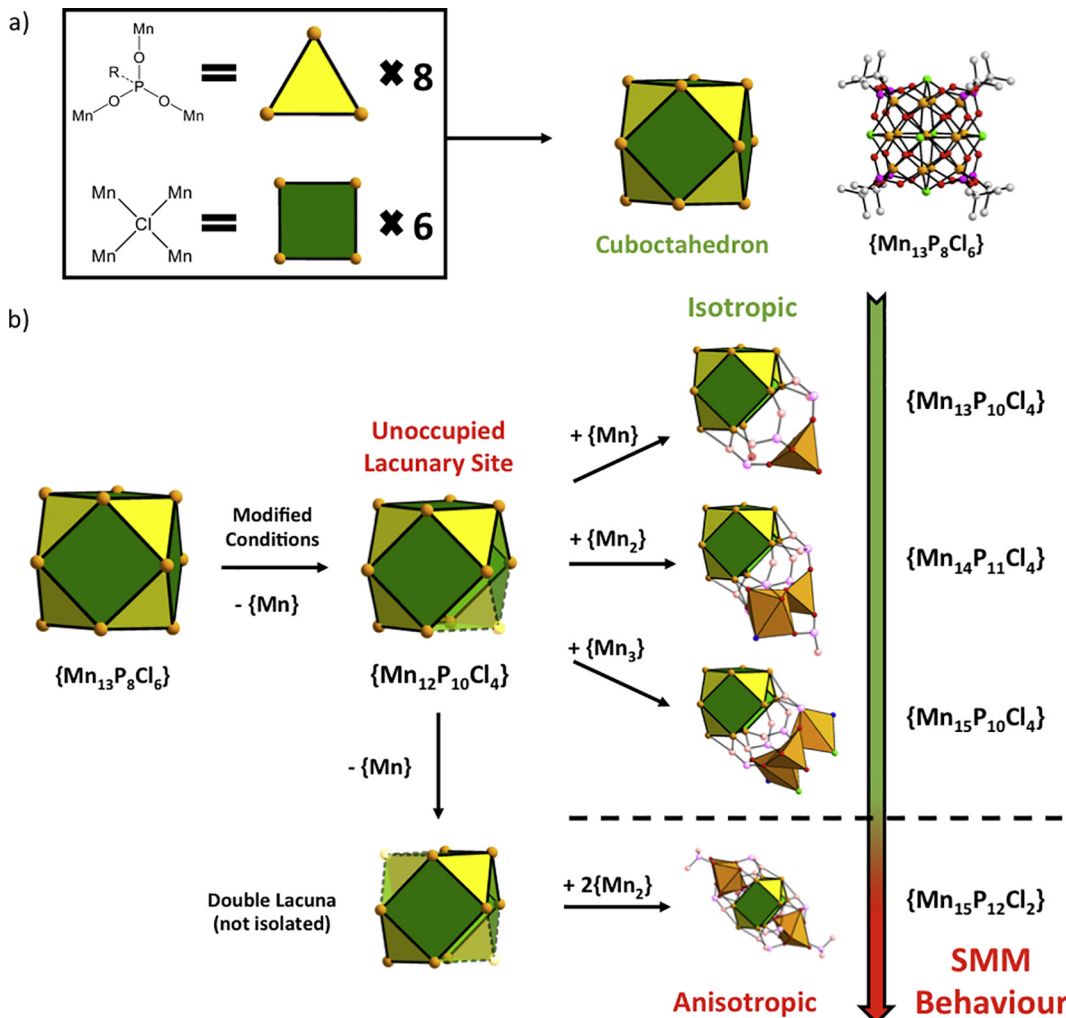


Fig. 8. a) The combination of $[M_4X]$ capped square motifs with triangular phosphonate ligands can generate the Archimedean Cuboctahedron geometry, exemplified by a $\{Mn_{13}P_8Cl_6\}$ species. b) Modification of the reaction conditions can generate lower-symmetry analogues of this structure. These can be conceptualised as removing one Mn centre to generate a lacunary structure and introducing zero, one, two or three Mn centres into the lacunary site to generate $\{Mn_{12}P_{10}Cl_4\}$, $\{Mn_{13}P_{10}Cl_4\}$, $\{Mn_{14}P_{11}Cl_4\}$ or $\{Mn_{15}P_{10}Cl_4\}$ species. Further modification of the structure generates a $\{Mn_{15}P_{12}Cl_2\}$ species which is sufficiently anisotropic to display single molecule magnet (SMM) behaviour [130,131].

$PO_3)_{10}(MeO)_6(picoline)_4^{0.5+}$, can be isolated [132]. This system is extremely distorted, but retains the cuboctahedron topology by expanding the coordination modes of six of the phosphonate ligands to $\{4.2.11\}$ binding modes to generate the (distorted) square faces. Four of the triangular faces are capped by the remaining phosphonates in $\{3.111\}$ binding modes, with the remaining four triangular faces remaining uncapped. It was demonstrated that the labile terminal picoline and methanol ligands on the structure could be displaced by bridging linker ligands, generating supramolecular polymer systems. Moreover, the use of a redox-active linker ligand tetracyanoquinodimethane (TCNQ) simultaneously connects the coordination cluster into a supramolecular polymer while influencing the oxidation state of the central manganese atom, significantly affecting the magnetic properties of the system.

Thus the presented class of manganese coordination compounds with cuboctahedral topology demonstrates a metallo-supramolecular principle, whereby relatively simple templates (triangles and squares) can be combined to generate structurally complex, high nuclearity species. Moreover, lower symmetry and chiral analogues can be generated, effectively introducing SMM behaviour into the complexes by simply perturbing the balance

of structure-directing templates bound to the complexes. Importantly the compound retain their structural integrity in organic solvents such as acetonitrile or methanol, allowing mass spectrometry to be applied to monitor the transformations between individual structures.

4.2.3. Vanadates

The $\{M_4X\}$ capped square motif is also common in an important class of compounds, the vanadates. Vanadates are somewhat distinct in their chemistry from other first row transition metals, belonging to set of compounds known as polyoxometalates (POMs) [133]. Templating and structure directing effects like those discussed above are foundational concepts in POM chemistry [134], but POMs are classically supported by only oxo-ligands and oxo-anions (although strategies do exist to incorporate organic ligands or heteroatoms into the structures [135,136]). However, unlike other POMs, vanadates can form square pyramidal $\{VO_5\}$ oxo-units [133]. It has been shown that non-oxo anions and nucleophiles (including halides and pseudohalides) can donate to the σ^* orbitals of the terminal V = O double bond in the $\{VO_5\}$ units, allowing non-oxo anionic template species to be incorporated into vanadate structures [137–140].

The $\{V_4X\}$ capped square motif is particularly common in vanadate species (Fig. 9). The $\{V_4X\}$ motif is usually stabilised by four terminal $V=O$ oxo-ligands (one on each metal centre) and by ligands which bridge along the sides of the square. In fully oxidised (V^V) species, four bridging oxo-ligands are most common, while in reduced (V^{IV}) species $\{PO_4\}$ or $\{AsO_4\}$ units can bridge between the metal centres by binding to the opposite face from the halide. Like the $\{M_4X\}$ squares described above, the $\{V_4X\}$ motif is usually additionally stabilised along each edge by peripheral bridging ligands such as carboxylates, phosphonates or arsonates (Fig. 9b). While

this motif can be isolated using capping organic ligands [141,142], structurally complex structures can be generated using bridging ligands.

One family of vanadate compounds containing the $\{V_4X\}$ capped square motif is the set of capsule vanadates (Fig. 10). In these compounds, two square vanadate units are supported by four peripheral phosphonate or arsonate ligands. The dangling O-donors from these ligands can then coordinate to a vanadate “belt” to generate a capsule structure. The coordination modes around these bridging vanadate units determines the overall size and

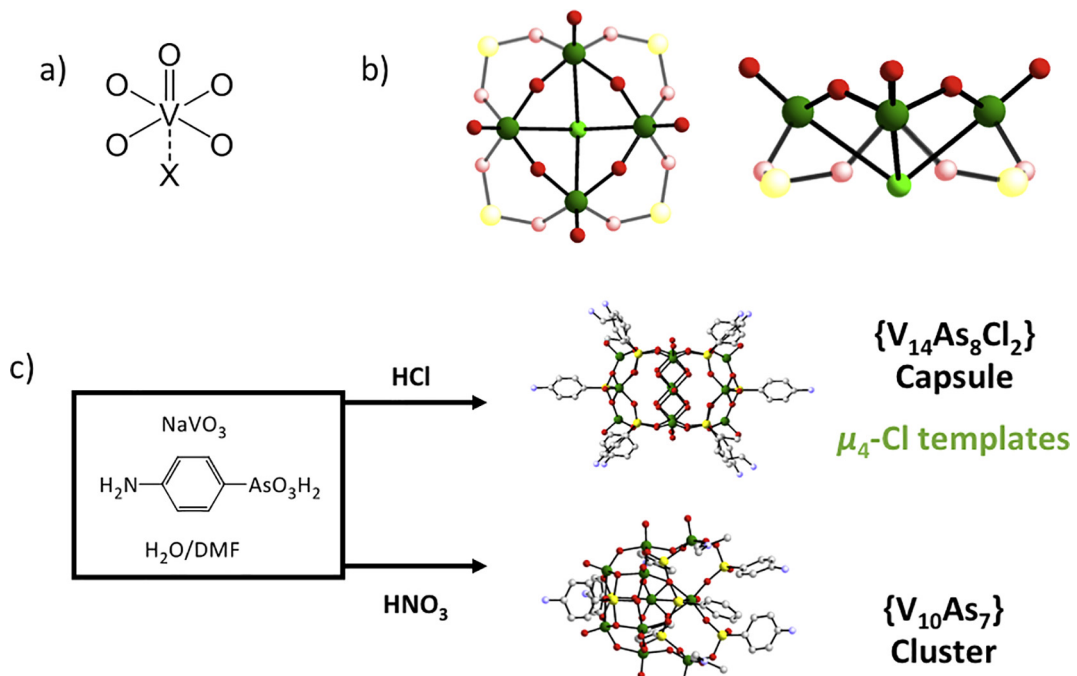


Fig. 9. a) Anionic (non-oxo) species can interact with square pyramidal $\{VO_5\}$ units via weak coordination bonds. b) This can result in the common $\{V_4X\}$ motif. The peripheral ligands are partially shaded. The unit may also be capped by $\{RPO_4\}$ or $\{RPO_3\}$ units in place of the four bridging oxo-ligands. c) Illustration of structure-directing effects in vanadate synthesis. Under identical synthetic conditions, the presence of chloride generates a $\{V_{14}As_8Cl_2\}$ capsule, while nitrate generates a $\{V_{10}As_7\}$ cluster [142,146].

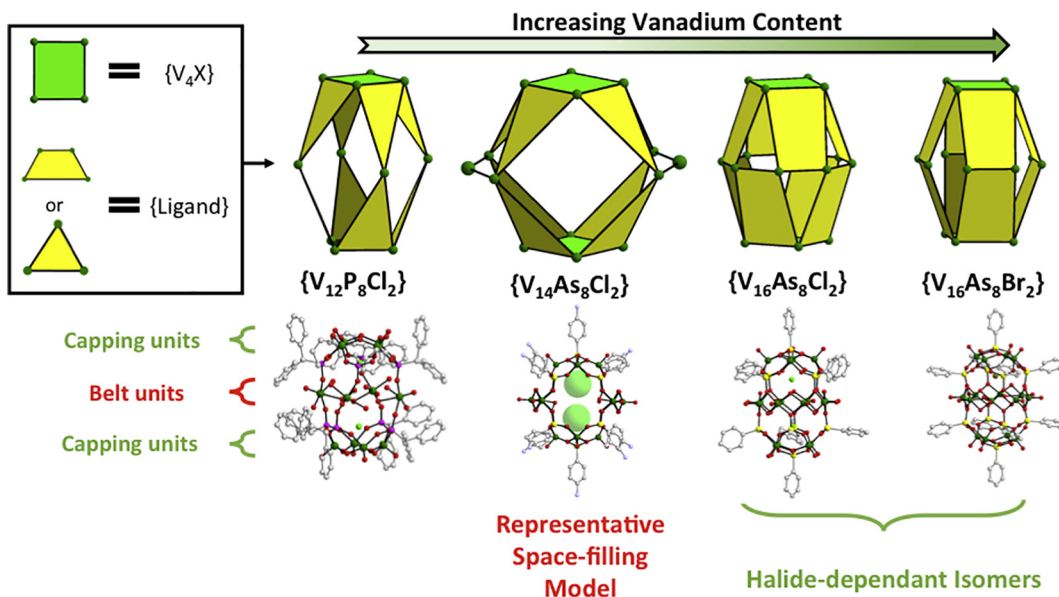


Fig. 10. Various vanadate capsule molecules based on the $\{V_4X\}$ motif and either phosphonate or arsenate ligands. The geometry of the bridging ligands and nuclearity of the belt units determine the size and shape of the cavity, which is occupied by the halide template units as well as water molecules [144,146,147].

geometry of the capsule. In the simplest example of this principle, two of these $\{V_4X\}$ units can be combined with triangular phosphonate or arsonate ligands and a $\{V_4\}$ belt to generate $\{V_{12}\}$ capsules [143–145]. Additional vanadate units can be added to the belt unit to generate a closely related $\{V_{14}\}$ species [146]. In each case, the capsule units are filled by the templating halides and water molecules. The importance of the chloride template was demonstrated in the case of the $\{V_{14}\}$ species, where replacement of chloride with nitrate in the reaction mixture generated an unrelated $\{V_{10}\}$ species (see Fig. 9c) [146].

The capsule systems can be further expanded by expanding the coordination mode of the capping ligands. In the {4.211} binding mode, arsonate ligands approximate a trapezoidal geometry, allowing each arsenate ligand coordinating to two vanadates in a $\{V_8\}$ belt unit to generate a $\{V_{16}\}$ species. Interestingly, two isomers of this capsule can be generated, based on whether the templating halide is a chloride or bromide (Fig. 10) [147]. Depending on which halide is used, the capping units can be twisted by 45° with respect to each other to generate two distinct isomers. The well-defined geometry of the peripheral arsonate ligands offers a potential building unit in extended architectures, with the halide-dependent isomerism giving a degree of control over the building unit geometry [147].

The trapezoidal arsonate template can be used in conjunction with four $\{V_4Cl\}$ units to generate a toroidal $\{V_{16}\}$ structure (Fig. 11) [147]. Interestingly, linking units can be added across the void in the centre of the toroidal structure by expanding the coordination mode of the arsenate ligands. A mixed-valent $\{V_{20}\}$ structure can be generated by adding two $\{V_2\}$ units across this structure. These $\{V_2\}$ units are connected to the structure by the arsonate ligands, which have expanded their coordination modes to the {5.221} distorted pentagon binding mode [147]. This cage structure is also filled by templating halide and water molecules. Finally, by expanding the arsenate binding modes to {6.222}, a $\{V_{24}\}$ structure can be generated using the same methodology. This structure can alternately be understood as a truncated octahedron constructed from 6x $\{V_4Cl\}$ squares and 8x{arsonate} hexagons, or as the $\{V_{16}\}$ toroidal structure capped by two additional $\{V_4Cl\}$ units. This cage structure contains only halide template ions, which form a $\{Cl_6\}$ octahedron with Cl–Cl distances of approximately 4 Å.

While the versatility in coordination mode of arsenates offers synthetic flexibility, the coordination mode can be difficult to predict from first principles. Therefore, using the strategy above with more well-defined linker ligands should give more synthetic control over the geometry of the resulting compounds. This was demonstrated by Zaworotko et al. in 2014 using benzenetricarboxylate (BTC) linker ligands (which approximate to distorted hexagons) to connect $\{V_4Cl\}$ units to generate distorted truncated octahedral structures. These molecular cage structures contain large void spaces, and were termed “hyballs” (hybrid balls) for their organic-inorganic nature (Fig. 12) [148]. The relatively longer linkers generated intrinsic voids imparted a permanent porosity to the system. This allowed the hyballs to be investigated for gas sorption analyses [148]. Further, the hyball systems could be cross-linked via intermolecular interactions including hydrogen bonding and electrostatic interactions to generate extended network structures [148].

The well-defined binding modes of the BTC ligand allow for rational modification of this structure. The following year, Zaworotko et al. reported the same $\{V_4Cl\}$ assembly strategy, but with one carboxylate position on the BTC ligand replaced (with –H, –Br or –OMe substituents) [149]. The removal of one carboxylate moiety effectively generates an approximately trapezoidal ligand, which alters the resulting vanadate structure from a truncated octahedron to a toroidal structure (termed a “hydoughnut”, or hybrid doughnut) [149]. The authors propose that these hydoughnut structures could be used in host guest chemistry or assembled into extended networks in a similar fashion to the hyball systems.

5. Structure-directing μ_5 -halide ions

A closely related unit to the $\{V_4X\}$ unit described above is the $\{V_5X\}$ unit. As mentioned above, when the $\{V_5X\}$ unit is in a lower oxidation state (i.e. V^{IV}), it can be stabilised by $\{RAsO_4\}$ or $\{RPO_4\}$ units, which bridge between the V atoms by coordinating opposite to the halide ion. The $\{V_5X\}$ unit can be understood as a $\{V^VO_5\}$ unit coordinating in place of these $\{RAsO_4\}$ or $\{RPO_4\}$ moieties (Fig. 13a). This assembly is then similarly stabilised by peripheral ligands which bridge along the square edges of this structural syn-

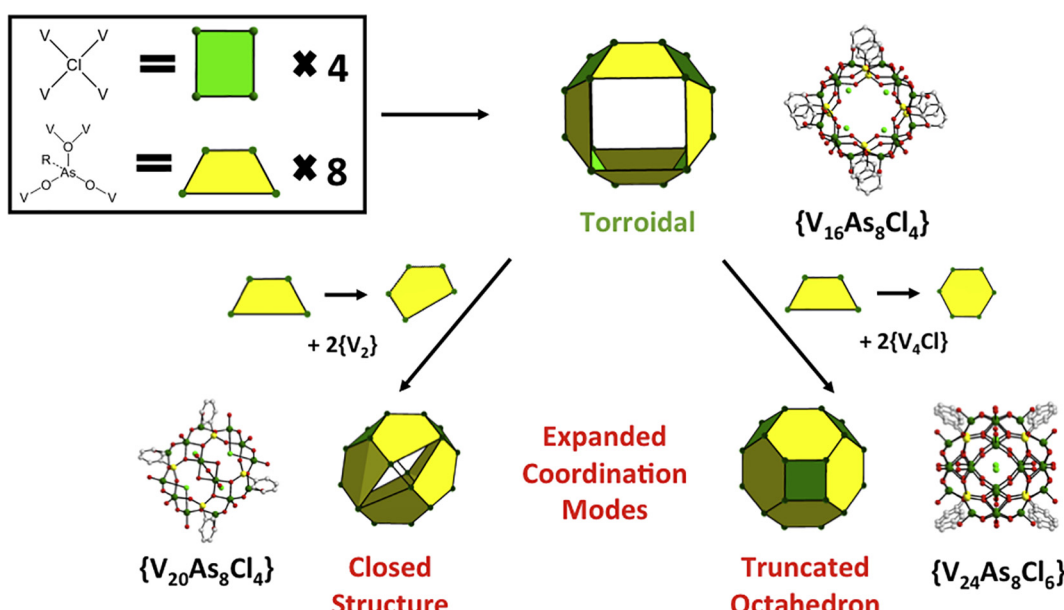


Fig. 11. The combination of four $\{V_4Cl\}$ units with eight arsenate ligands in trapezoidal coordination modes generates an approximately toroidal $\{V_{16}As_8Cl_4\}$ structure. Further expansion of the arsenate coordination modes generates $\{V_{20}As_8Cl_4\}$ and $\{V_{24}As_8Cl_6\}$ structures [147].

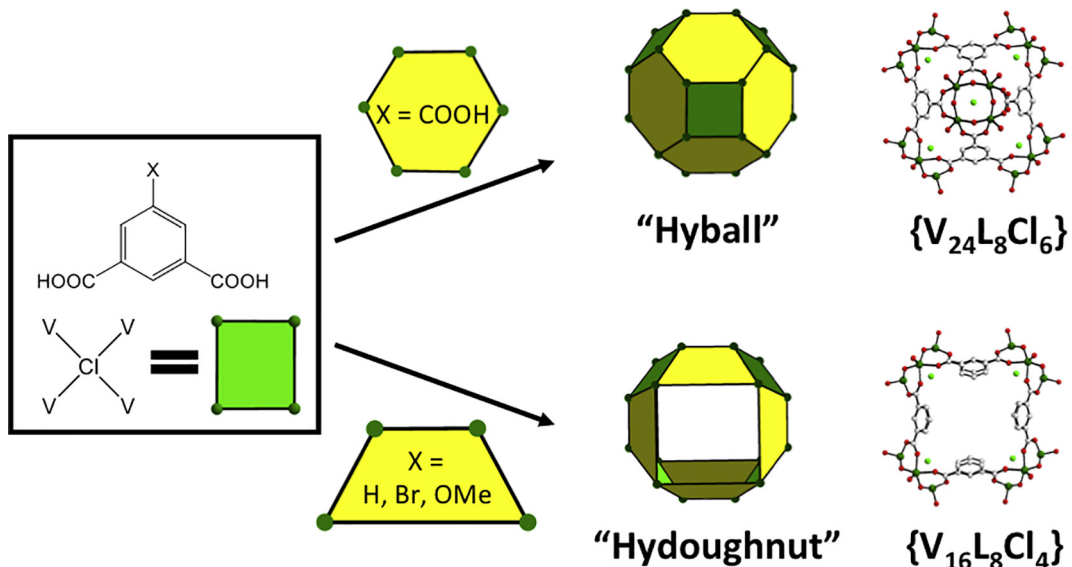


Fig. 12. Benzenetricarboxylate (BTC) in conjunction with the $\{V_4Cl\}$ motif generates truncated octahedron structures (“hybrid balls”), while blocking one carboxylate moiety (with $-H$, $-Br$ or $-OMe$ moieties) the toroidal “hybrid doughnut” structure [148,149].

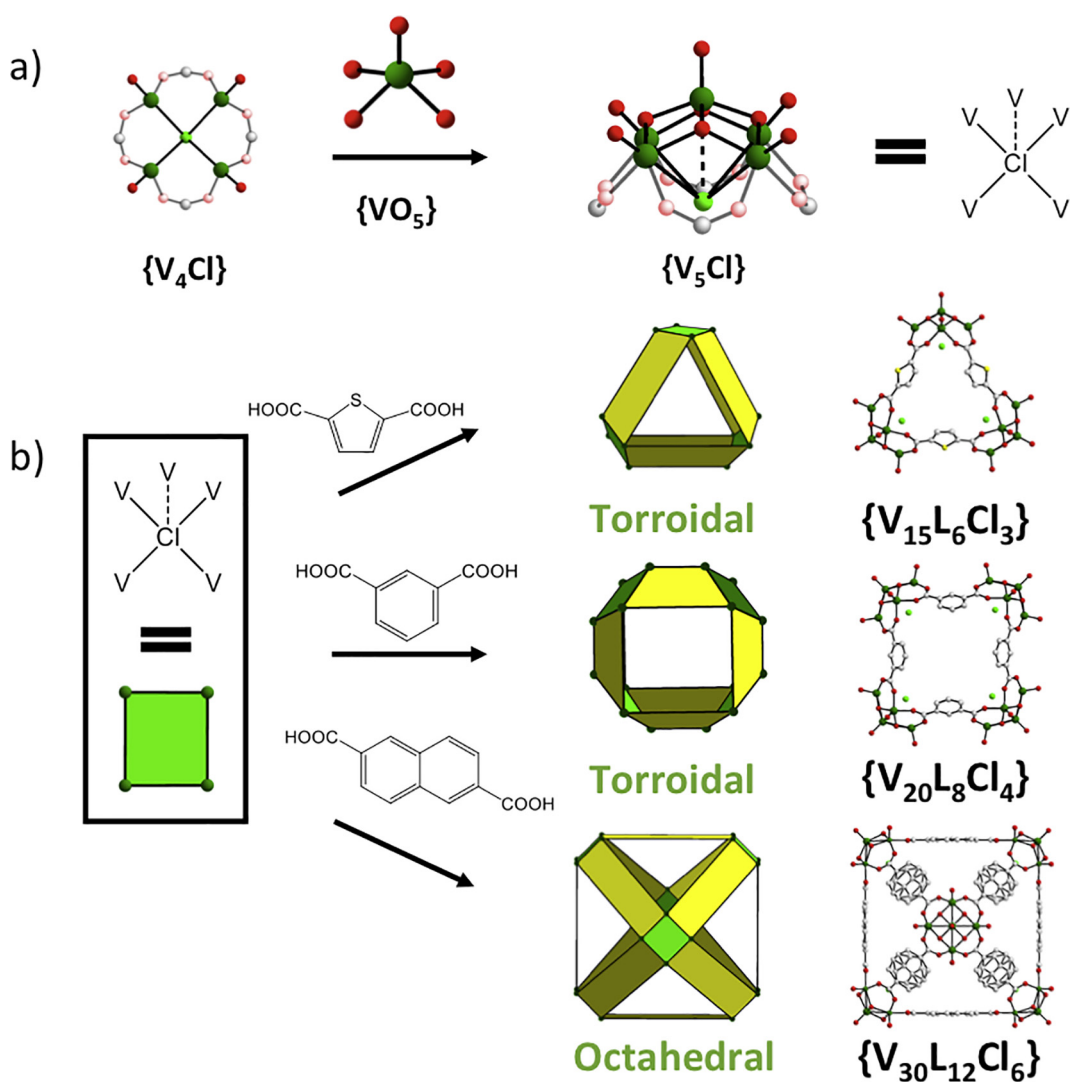


Fig. 13. a) the $\{V_5X\}$ motif can be understood as a $\{V_4X\}$ motif capped by an additional $\{VO_5\}$ unit. b) The $\{V_5Cl\}$ unit was used in conjunction with a series of dicarboxylate linkers of different geometry to generate $\{V_{15}\}$, $\{V_{20}\}$ and $\{V_{30}\}$ hybrid structures [152].

thon. Examples of this motif have been prepared using both chloride and bromide templates, and simple carboxylates including acetate or benzoate ligands to stabilise the unit as an isolated molecule [150,151].

As expected, the $\{V_5X\}$ unit behaves very similarly to the $\{V_4X\}$ described in the previous section. For example, the “hyball” systems described in Fig. 12 can be generated using either $\{V_4Cl\}$ or $\{V_5Cl\}$ units through simple modifications of the reaction system [148].

This methodology of linking $\{V_5Cl\}$ units with polycarboxylate linkers was expanded in 2016 with a series of impressive structures presented in 2016 (Fig. 13). Variable dicarboxylate linkers with distinct binding angles were used to generate structures of different nuclearity [152]. Simple isophthalate ligands generate the $\{V_5Cl\}$ analogue of the hydoughnut system presented in the previous section, as expected. However, a bent thiophene dicarboxylate linker generated a $\{V_{15}\}$ truncated triangular structure, which represents the first reported example of a trimeric vanadate metal-organic polyhedron [152]. Meanwhile, moving to a linear naphthalene dicarboxylate linker generated an intriguing $\{V_{30}\}$ structure with truncated octahedral topology [152]. Ferromagnetic interactions between the V^{IV} centres dominate the magnetic properties of these compounds [152].

Although templating nucleophiles (including halides and pseudohalides) seem important for the formation of $\{V_4X\}$ and $\{V_5X\}$ units [137–140], the structure-directing agents can be displaced while leaving the units intact. This strategy was exploited to generate cage structures using linear diphosphonate ligands to bridge between two $\{V_5\}$ units [144,145]. These cage structures contain only solvent molecules. This may simply be due to a size effect – extending the linker length can generate cages sufficiently large to contain two pseudohalide (N_3^-) templates [153]. Again, ferromagnetic interactions between the V^{IV} ions dominate the magnetic properties [144,145]. The same template displacement approach

can also be applied to generate isolated $\{V_4\}$ complexes and $\{V_{12}\}$ capsules [144,145].

6. Structure-directing μ_6 -halide ions

Hexacoordinate halide ions represent particularly interesting structure-directing agents. In the most common μ_6 -halide-templated coordination compounds, a central ligand species occupies the centre of an octahedron whose vertices are composed of metal atoms. Thus this $\{M_6X\}$ motif represents an inversion of the familiar $\{MX_6\}$ octahedral coordination environment. This “inverted octahedron” can be generated using manganese (III) ions and a chloride or bromide template [154,155]. This arrangement is geometrically suitable for eight phosphonate ligands to bind to the metal centres, with each phosphonate O-donor coordinating in a {3.1.1.1} mode, effectively capping the faces of the halide-templated octahedron (Fig. 14) [154].

The coordination environments of the manganese (III) centres are completed by terminal O-donors or N-donors, which occupy the Jahn-Teller axes of the respective metal centres, in a *trans*-position relative to the halide ion. Use of bifunctional ligands such as 4,4'-bipyridine can link the octahedral $\{M_6X\}$ units into extended structures including polymer chains [154]. Supramolecular π - π stacking interactions can also lead to the formation of gel-like aggregates (Metal-Organic Gels, or MOGs) constructed from the $\{M_6X\}$ octahedral motif. These gels can be destroyed by mechanical agitation, but will spontaneously reform from solution (Fig. 14) [154].

Analogous compounds can also be generated using vanadyl ($V = O$) in place of the manganese (III) centres [156–158]. In this case, the capping ligand can be either *tert*-butyl- or phenyl-phosphonate, with either a chloride or bromide as a central template [156,157]. A similar motif can be obtained using triangular tris-alkoxide ligands and a central fluoride template, but in this

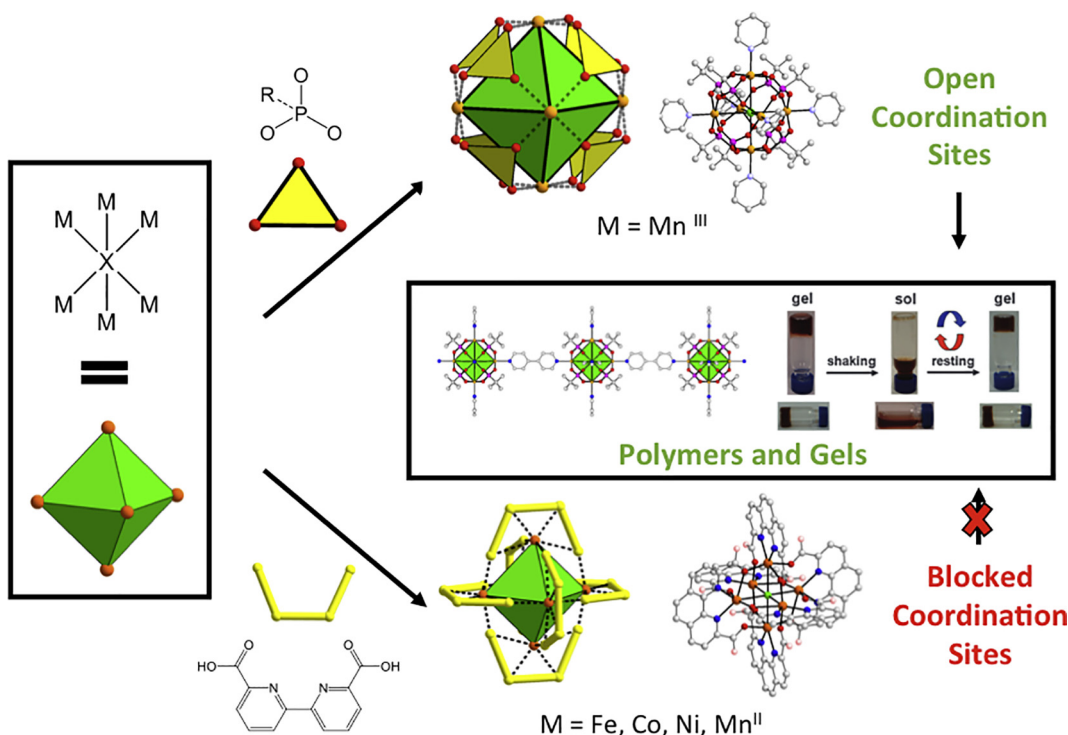


Fig. 14. The $\{M_6X\}$ “inverted octahedron” motif can be stabilised by a variety of ligands, including phosphonate ligands (top) and capping phenanthrolinediacetate (phenda) ligands (bottom). The phosphonate stabilised motif possesses open coordination sites which can be used to generate extended structures (polymers and gels), while the capping phenda ligands block these sites and prevent further aggregation [154,160,161].

instance the cage distorts significantly, with the fluoride displaying shorter bonds to three of the vanadate centres (*c.* 2.25 Å) when compared to the other three (*ca.* 2.50 Å) [158]. Based on crystallographic evidence, in one report, the authors proposed that the outer {V₆} cage structure can also form around OH⁻ or {HCl} units [157].

Chemical reduction of the manganese (III) system to manganese (II) removes the significant Jahn-Teller distortion from the metal centres, effectively shortening the M-X distance [159]. This arrangement can be stabilised by twelve pivalate ions, which each ligand capping one edge of the {M₆X} octahedral motif [159]. In this instance, the pivalate ligands coordinate asymmetrically in {2,21} binding modes, making each manganese centre seven-coordinate.

The most successful strategy for generating the octahedral {M₆X} motif is by using 1,10-phenanthroline-2,9-dicarboxylate (*phenda*) capping ligands. These capping ligands were first used independently in 2010 by Miao et al. and Chen et al. to generate iron (II) and cobalt (II) examples, but the series has since been expanded to include manganese (II) and nickel (II) compounds [160–162]. In these systems, each ligand caps two adjacent edges of the octahedral motif, coordinating to one metal centre with two N-donors and bridging between this metal centre and two adjacent metal centres with the O-donors [160–162]. Magnetic susceptibility measurements were conducted for all of these *phenda* compounds, with predominantly antiferromagnetic interactions dominating the systems. In the case of cobalt (II), it was shown that the central halide ion can be either chloride or fluoride, but the motif could not be generated around bromide or iodide templates [161]. At low temperatures, the chloride and fluoride templates had significant effects on the magnetic exchange between metal centres.

In the manganese-pivalate system and the *phenda*-supported systems, each metal centre is seven-coordinate, effectively blocking any additional ligands from coordinating to the metal centres. In the vanadyl systems, the terminal V=O bonds are extremely stable and so the terminal oxo-ligand cannot be readily replaced. Thus, only in the manganese (III) phosphonate system is there a ligand which is sufficiently labile to be replaced while retaining the core structure. Thus, only this system can be modified to generate polymer and gel systems, while the others remain as coordinatively saturated molecular species (Fig. 14).

A final μ_6 -halide-templated motif to be mentioned is the {M₆X} “barrel” motif, in which six metal atoms form a planar ring around the central halide template [163–166]. This motif is generally stabilised by a macrocyclic organosiloxanolate ligands, which cap above and below the {M₆X} ring to generate the barrel structure [163–166]. First reported in 1992 with manganese, cobalt, nickel and copper examples [163], investigations into mixed-metal analogues of the barrel motif were carried out over the subsequent decade [164–166]. The barrel motif re-emerged in 2011 with the isolation of a {M₆X} ring structure, [Cl \subset Cu₆^{II}(OH)₆(L)₆]⁻, where L represents pyrazole ligands [167]. The pyrazole and hydroxide ligands alternate around the ring, generating a “double calix” structure. The structure was investigated for host-guest chemistry, with the hydroxide and chloride-lined cavities formed a complementary hydrogen bonding pocket for chloroform [167]. Moreover, the pyrazole ligands extended in a well-defined trigonal antiprism, allowing the copper units to be connected into extended framework structures *via* the incorporation of linking cadmium ions [167].

7. Larger entities

Few examples of larger halide-templated polynuclear assemblies (*i.e.* {M_nX} species where n > 6) exist for first-row transition

metal ions. Steric crowing and Coulombic repulsion between the metal centres prevent such large numbers of metal centres aggregating around a single anion. However, the vanadates represent a significant exception to this principle. Many examples of high nuclearity vanadates with encapsulated anions exist, including halides, pseudohalides, nitrates, *etc.*, with the shape of the encapsulated ion influencing the shape of the clusters [133,140,168,169]. In mixed-valence examples of these large vanadate clusters, charge delocalisation between the metal centres is common, giving rise to interesting electronic and magnetic behaviour [169,170].

The obvious question is how such small templating species could generate such large cluster species. Indeed, in the case of one {V₁₂Cl} capsule, it has been demonstrated by DFT calculations that the chloride effectively offers zero stabilisation to the cluster – the stabilisation offered by Cl-V interactions is almost exactly cancelled out by the Cl-O repulsion [171]. In cases such as this, the template does not stabilise the cluster *per se*; instead, the anion is important for the initial stages of aggregation, templating a concave vanadate structure (*c.f.* the {V₄X}, {V₅X} and {V₆X} species described above) [137–140]. Subsequent growth and aggregation of vanadate fragments continues in a concave fashion, and although the anion offers less and less to the cluster in terms of stabilisation, the halide is effectively trapped inside a growing cage structure (Fig. 15). The overall result is a large “anion templated” vanadate cage with very little V-X interaction [133,168].

In the large family of vanadate clusters, {V₁₂X} clusters offer a particularly interesting set of compounds. [V₁₂O₃₂Cl]⁵⁻ can exist in one of several isomers – the closed, tube, and open isomers [172–174]. The “open” isomer represents a bowl-shaped cluster, which can incorporate anionic guests into the central cavity [175,176]. In this configuration, one face of the guest anion is exposed so it can interact with other species in solution. This was exploited in one instance to generate an “empty bowl” species by precipitating AgCl from solution. Upon re-addition of chloride to the solution, the empty bowl system was shown to recapture chloride into its cavity [172]. In the closed isomer [174], however, the central chloride is sufficiently shielded from solution and so it cannot be removed by precipitation as a silver salt [172]. The open and closed isomers can be interconverted, apparently proceeding via the tube isomer [172].

The tube isomer of the {V₁₂Cl} cluster represents a particularly interesting unit in POM chemistry [171,177]. This cluster has a ring-like structure around the central chloride ion. On either side of the ring there are two “lacunary sites”, with multiple oxo-ligands arranged in a favourable configuration to bind heterometals. Adding heterometals into lacunary sites is a common strategy to generate mixed-metal POM units, but in this instance there are two distinct lacunary sites on the same molecule.

Demonstrating a remarkable degree of synthetic control over the formation of heterometallic POM systems, Streb et al. used ammonium cations to “block” these lacunary sites – subsequent displacement of the ammonium cations allowed the authors to generate mono- or di-substituted vanadate systems in a controlled, stepwise manner [171,177]. Fe, Co, Mn, Cu and Zn substituted analogues of the {V₁₂Cl} unit have been generated. Initial catalytic tests indicated that both the mono- and di-substituted manganese analogues were competent catalysts for oxidative C–H activation reactions [177]. Further catalytic tests would be extremely interesting, especially considering the unusual degree of control over heterometal substitution. Magnetically and optically interesting lanthanide ions can also be incorporated at either one or both of the lacunary sites of the {V₁₂Cl} tube isomer [178,179].

Although the central halide is in principle a passive prisoner inside the vanadate cage, halide substitution can still have a significant impact on the chemistry of the clusters. Streb et al. presented

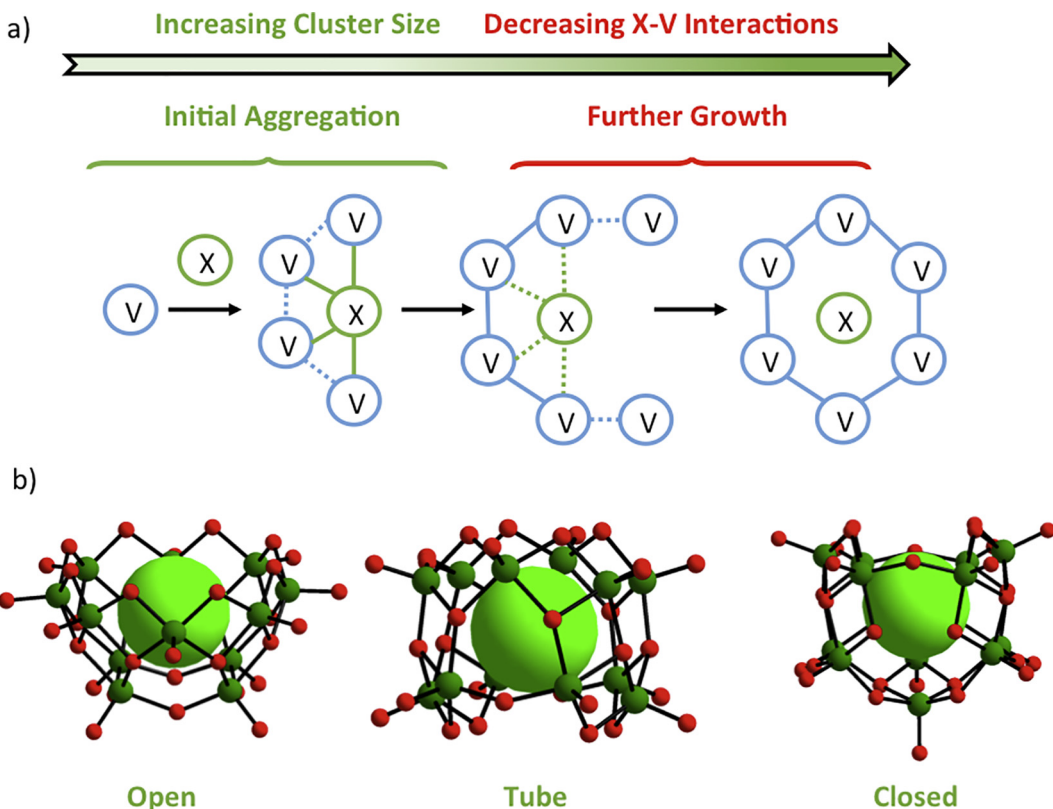


Fig. 15. a) Anion templates are often important for the initial templating of concave vanadate clusters, but as these clusters grow the vanadate-anion interaction tends to decrease. This can result in vanadate cage structures with an anionic guest molecule trapped inside, which does not necessarily contribute to the stability of the cluster. b) The open, tube, and closed isomers of the $\{V_{12}O_{32}X\}$ structure [133,172].

two isostructural bismuth-substituted $\{V_{12}X\}$ clusters, $[X(Bi(DMSO)_3)_2V_{12}O_{33}]^-$, and examined their activity as photocatalysts for oxidative dye degradation [180,181]. Despite the weak interactions between the halide and vanadate, a significant increase in activity was seen for the bromide case. This is attributed to the heavy atom effect of the bromide, which facilitates more efficient singlet-triplet transitions in the excited state photocatalyst [180].

The $\{V_{12}O_{32}X\}$ structure can also be generated with cerium ions at the lacunary sites in place of bismuth. These compounds were also shown to be active for the photocatalytic oxidation of dye molecules [182]. Importantly, the $\{V_{12}O_{32}X\}$ structure is chiral, which the authors suggest might allow for asymmetric photocatalytic oxidations.

Vanadate structures with higher nuclearity are also possible. A $[V_{14}O_{36}Cl]^{5-}$ cluster has a “flower basket” structure, with a concave basket unit topped by a bridging “handle”. Interestingly, this cluster exhibits strong blue luminescence, which is relatively unusual. The authors postulate that this arises from a strong LMCT absorbance band in the UV [183]. Meanwhile, a closed-shell $\{V_{14}Cl\}$ cluster, $[V_{14}O_{38}Cl]^{7-}$, can be generated from a rearrangement reaction of the open isomer of the $[V_{12}O_{32}Cl]^{5-}$ system [173].

A $\{V_{15}Cl\}$ cluster, $[V_{15}O_{36}Cl]^{6-}$, represents a “closed shell” vanadate structure, and was one of the earliest reported halide-templated vanadate structures. The cluster is formally designated as a $\{V_7^VI V_8^{IV}\}$ system, but charge delocalisation occurs between the metal centres [184]. Since the initial report, analogues of this cluster have been reported in a variety of oxidation states. These analogues are generally prepared as solid-state composites with a variety of cationic species, with a focus on structural and magnetic studies [185–190]. The $\{V_{16}Cl\}$ cluster is similar, with studies again focusing

on structural aspects of solid-state composites [38,189–192]. $\{V_{16}\}$ clusters can also be generated with fluoride or bromide templates [189].

8. Conclusions

In conclusion, relatively simple structure-directing agents can be used to generate complicated coordination compounds by combining multiple templates to generate a sophisticated, well-defined architectures. Templating species bias a coordination compound towards a particular geometry, with simple templates generating polynuclear entities with simple geometries (triangles, squares, hexagons, etc.). However, when multiple templating species are used in combination, much more interesting species can be obtained, with geometries resembling Platonic and Archimedean solids and beyond. Cage structures, framework structures, and giant molecular structures (among others) can be predicted and rationalised using this simple approach of combining multiple structure-directing agents. The complexity of structures that can be generated from simple templates allows a wide range of applications to be accessed, including catalysis, magnetism, and host-guest chemistry.

This review focussed on the structure-directing effects of halide templates – although the principles explored here are applicable to a much wider array of structure-directing agents. Halides can generate simple triangle and square units, Platonic and Archimedean solids, cubanes, supertetrahedra, shuttlecock motifs, nano-assemblies, frameworks, and hybrid cage structures – simply through combination with suitable complementary structure-directing agents.

We hope that this review was able to elucidate some of the structural motifs generated by simple template species, and how simple building principles can generate remarkable coordination compounds by exploiting multiple template effects in concert with one another.

Declaration of interest

The authors declare no competing interests.

Acknowledgements

The authors thank Science Foundation Ireland (SFI; 13/IA/1896), the European Research Council (CoG 2014 – 647719) and the Irish Research Council (Fellowship for C.H.) for financial support. The authors also thank Paul Wix and Swetanshu Tandon for valuable comments and Friedrich Steuber for translation services.

Appendix A. Supplementary data

Supplementary data associated with this article can be found, in the online version, at <https://doi.org/10.1016/j.ccr.2018.05.014>.

References

- [1] B. Hasenknopf, J.-M. Lehn, N. Boumediene, A. Dupont-Gervais, A. Van Dorsselaer, B. Kneisel, D. Fenske, Self-assembly of tetra- and hexanuclear circular helicates, *J. Am. Chem. Soc.* 119 (1997) 10956–10962.
- [2] J.J. Danon, A. Krüger, D.A. Leigh, J. Lemonnier, A.J. Stephens, I.J. Vitorica-Yrezabal, S.L. Woltering, Braiding a molecular knot with eight crossings, *Science* 355 (2017) 159–162.
- [3] J.-F. Ayme, J.E. Beves, D.A. Leigh, R.T. McBurney, K. Rissanen, D. Schultz, A synthetic molecular pentafoil knot, *Nat. Chem.* 4 (2012) 15–20.
- [4] V. Marcos, A.J. Stephens, J. Jaramillo-Garcia, A.L. Nussbaumer, S.L. Woltering, A. Valero, J.-F. Lemonnier, I.J. Vitorica-Yrezabal, D.A. Leigh, Allosteric initiation and regulation of catalysis with a molecular knot, *Science* 352 (2016) 1555–1560.
- [5] Y. Li, K.M. Mullen, T.D.W. Claridge, P.J. Costa, V. Felix, P.D. Beer, Sulfate anion templated synthesis of a triply interlocked capsule, *Chem. Commun.* 7134–7136 (2009).
- [6] K. Pandurangan, J.A. Kitchen, S. Blasco, E.M. Boyle, B. Fitzpatrick, M. Feeney, P. E. Kruger, T. Gunnlaugsson, Unexpected self-sorting self-assembly formation of a [4:4] Sulfate: ligand cage from a preorganized tripododal urea ligand, *Angew. Chem. Int. Ed.* 54 (2015) 4566–4570.
- [7] A. Ferguson, M.A. Squire, D. Siretanu, D. Mitcov, C. Mathoniere, R. Clérac, P.E. Kruger, A face-capped $[Fe4L4]^{8+}$ spin crossover tetrahedral cage, *Chem. Commun.* 49 (2013) 1597–1599.
- [8] S.R. Halper, L. Do, J.R. Stork, S.M. Cohen, Topological control in heterometallic metal – Organic frameworks by anion templating and metalloligand design, *J. Am. Chem. Soc.* 128 (2006) 15255–15268.
- [9] K. Wei, J. Ni, J. Gao, Y. Liu, Q.-L. Liu, Self-assembly of silver (I) coordination polymers from AgX and a rigid bent 3,6-dicyano-9-phenylcarbazole ligand, *Eur. J. Inorg. Chem.* 3868–3880 (2007).
- [10] T. Friščić, D.G. Reid, I. Halasz, R.S. Stein, R.E. Dinnebier, M.J. Duer, Ion- and liquid-assisted grinding: improved mechanochemical synthesis of metal – Organic frameworks reveals salt inclusion and anion templating, *Angew. Chem. Int. Ed.* 49 (2010) 712–715.
- [11] L. Liu, K. Konstas, M.R. Hill, S.G. Telfer, Programmed pore architectures in modular quaternary metal – Organic frameworks, *J. Am. Chem. Soc.* 135 (2013) 17731–17734.
- [12] R. Vilar, Anion-templated synthesis, *Angew. Chem. Int. Ed.* 42 (2003) 1460–1477.
- [13] N. Gimeno, R. Vilar, Anions as templates in coordination and supramolecular chemistry, *Coord. Chem. Rev.* 250 (2006) 3161–3189.
- [14] M.D. Ward, Polynuclear coordination cages, *Chem. Commun.* 4487–4499 (2009).
- [15] A.M. Castilla, W.J. Ramsay, J.R. Nitschke, Stereochemistry in subcomponent self-assembly, *Acc. Chem. Res.* 47 (2014) 2063–2073.
- [16] A. Caballero, F. Zapata, P.D. Beer, Interlocked host molecules for anion recognition and sensing, *Coord. Chem. Rev.* 257 (2013) 2434–2455.
- [17] G.T. Spence, P.D. Beer, Expanding the scope of the anion templated synthesis of interlocked structures, *Acc. Chem. Res.* 46 (2013) 571–586.
- [18] N.H. Evans, P.D. Beer, Progress in the synthesis and exploitation of catenanes since the Millennium, *Chem. Soc. Rev.* 43 (2014) 4658–4683.
- [19] M.J. Langton, P.D. Beer, Rotaxane and catenane host structures for sensing charged guest species, *Acc. Chem. Res.* 47 (2014) 1935–1949.
- [20] A.J. Tasiopoulos, A. Vinslava, W. Wernsdorfer, K.A. Abboud, G. Christou, Giant single-molecule magnets: a Mn₈₄ torus and its supramolecular nanotubes, *Angew. Chem. Int. Ed.* 43 (2004) 2117–2121.
- [21] L. Zhang, R. Clérac, C.I. Onet, C. Healy, W. Schmitt, Towards nanoscopic Mn-containing hybrid polyoxomolybdates: synthesis, structure, magnetic properties, and solution behavior of a Mn₆Mo₁₀ cluster, *Eur. J. Inorg. Chem.* 1654–1658 (2013).
- [22] G. Aromi, E.K. Brechin, Synthesis of 3d metallic single-molecule magnets, *Struct. Bond.* 122 (2006) 1–69.
- [23] R. Al-Oweini, A. Sartorel, B.S. Bassil, M. Natali, S. Berardi, F. Scandola, U. Kortz, M. Bonchio, Photocatalytic water oxidation by a mixed-valent manganese Oxo core that mimics the natural oxygen-evolving center, *Angew. Chem. Int. Ed.* 53 (2014) 11182.
- [24] B. Schwarz, J. Forster, M.K. Goetz, D. Yücel, C. Berger, T. Jacob, C. Streb, Visible-light-driven water oxidation by a molecular manganese vanadium oxide cluster, *Angew. Chem. Int. Ed.* 55 (2016) 6329–6333.
- [25] J. Soriano-López, S. Goberna-Ferrón, L. Vigara, J.J. Carbó, J.M. Poblet, J.R. Galán-Mascáros, Cobalt polyoxometalates as heterogeneous water oxidation catalysts, *Inorg. Chem.* 52 (2013) 4753–4755.
- [26] M. Blasco-Ahicart, J. Soriano-López, J.J. Carbó, J.M. Poblet, J.R. Galán-Mascáros, Polyoxometalate electrocatalysts based on earth-abundant metals for efficient water oxidation in acidic media, *Nat. Chem.* 10 (2018) 24–30.
- [27] Q. He, P. Tu, J.L. Sessler, Supramolecular chemistry of anionic dimers, trimers, Tetramers, and Clusters, *Chem.* 4 (2018) 1–48.
- [28] D. Sahoo, R. Suriyanarayanan, R.K. Metre, V. Chandrasekhar, Molecular and polymeric zinc(II) phosphonates: isolation of an octanuclear ellipsoidal ensemble, *Dalton Trans.* 43 (2014) 7304–7313.
- [29] J.E. Greedan, Geometrically frustrated magnetic materials, *J. Mater. Chem.* 11 (2001) 37–53.
- [30] E. Gao, N. Liu, A. Cheng, S. Gao, Novel frustrated magnetic lattice based on triangular $[Mn_3(\mu_3-F)]$ clusters with tetrazole ligands, *Chem. Commun.* 2470–2472 (2007).
- [31] N. Liu, Q. Yue, Y.-Q. Wang, A.-L. Cheng, E.-Q. Gao, Coordination compounds of bis(5-tetrazolyl)amine with manganese (II), zinc (II) and cadmium (II): synthesis, structure and magnetic properties, *Dalton Trans.* 4621–4629 (2008).
- [32] K.J. Anderton, D.M. Ermert, P.A. Quintero, M.W. Turvey, M.S. Fataftah, K.A. Abboud, M.W. Meisel, E. Čížmár, L.J. Murray, Correlating bridging ligand with properties of ligand-templated $[Mn_3X_3]^{3+}$ clusters, *Inorg. Chem.* 56 (2017) 12012–12022.
- [33] G.L. Guillet, F.T. Sloane, D.M. Ermert, M.W. Calkins, M.K. Peprah, E.S. Knowles, E. Čížmár, K.A. Abboud, M.W. Meisel, L.J. Murray, Preorganized assembly of three iron(II) or manganese(II) b-diketiminato complexes using a cyclophane ligand, *Chem. Commun.* 49 (2013) 6635–6637.
- [34] Y. Lee, K.J. Anderton, F.T. Sloane, D.M. Ermert, K.A. Abboud, R. García-Serres, L. J. Murray, Reactivity of hydride bridges in high-spin $[3M-3(\mu-H)]$ clusters, *J. Am. Chem. Soc.* 137 (2015) 10610–10617.
- [35] X. Bao, W. Liu, J. Liu, S. Gómez-Coca, E. Ruiz, M.-L. Tong, Self-assembly of pentanuclear mesocate versus octanuclear helicate, *Inorg. Chem.* 52 (2013) 1099–1107.
- [36] J. Qin, H.-R. Wang, Q. Pan, S. Zang, H. Hou, Y. Fan, Influence of ionic liquids on the syntheses and structures of Mn (II) coordination polymers based on multidentate N-heterocyclic aromatic ligands and bridging carboxylate ligands, *Dalton Trans.* 44 (2015) 17639–17651.
- [37] H. Sato, M. Yamaguchi, T. Onuki, M. Noguchi, G.N. Newton, T. Shiga, H. Oshio, Pentanuclear and octanuclear manganese helices, *Eur. J. Inorg. Chem.* 2193–2198 (2015).
- [38] Y. Teng, B. Dong, J. Peng, S. Zhang, L. Chen, L. Songa, J. Ge, Spontaneous resolution of 3D chiral hexadecavanadate-based frameworks incorporating achiral flexible and rigid ligands, *CrystEngComm.* 15 (2013) 2783–2785.
- [39] S. Langley, M. Hellwell, R. Sessoli, S.J. Teat, R.E.P. Winpenny, Synthesis and structural and magnetic characterization of cobalt (II) phosphonate cage compounds, *Inorg. Chem.* 47 (2008) 497–507.
- [40] S. Langley, M. Hellwell, R. Sessoli, S.J. Teat, R.E.P. Winpenny, Synthesis and structural and magnetic characterisation of cobalt (II)-sodium phosphonate cage compounds, *Dalton Trans.* 3102–3110 (2009).
- [41] S.K. Langley, M. Hellwell, S.J. Teat, R.E.P. Winpenny, Synthesis and characterisation of cobalt(II) phosphonate cage complexes utilizing carboxylates and pyridonates as co-ligands, *Dalton Trans.* 41 (2012) 12807–12817.
- [42] X. Zhang, T. Jiang, H. Wu, M. Zeng, Spin frustration and long-range ordering in an AlB₂-like metal-organic framework with unprecedented N,N,N-tris-tetrazol-5-yl-amine ligand, *Inorg. Chem.* 48 (2009) 4536–4541.
- [43] J.A. Armstrong, E.R. Williams, M.T. Weller, Cobalt(II) fluorophosphate frameworks, *Dalton Trans.* 41 (2012) 14180–14187.
- [44] S.R. Marri, S. Mahana, D. Topwal, J.N. Behera, Synthesis and characterization of layered metal sulfates containing $MII_3(\mu_3-OH/F)_2$ diamond chains, *Dalton Trans.* 46 (2017) 1105–1111.
- [45] S.A.K. Robinson, M.L. Mempin, A.J. Cairns, K.T. Holman, A. Cubic, 12-Connected, microporous metal – Organometallic phosphate framework sustained by truncated tetrahedral nodes, *J. Am. Chem. Soc.* 133 (2011) 1634–1637.
- [46] T.M. Powers, T.A. Betley, Testing the polynuclear hypothesis: multielectron reduction of small molecules by triiron reaction sites, *J. Am. Chem. Soc.* 135 (2013) 12289–12296.

- [47] S. Herold, S.J. Lippard, Synthesis, characterization, and magnetic studies of two novel isostructural pentanuclear iron (II) complexes, *Inorg. Chem.* 36 (1997) 50–58.
- [48] J.J.H. Edema, R. Duchateau, S. Gambarotta, C. Bensimon, Labile triangulo-trititanium(II) and trivanadium(II) clusters, *Inorg. Chem.* 30 (1991) 3585–3587.
- [49] D.L. Hughes, L.F. Larkworthy, G.J. Leigh, C.J. McGarry, J.R. Sanders, G.W. Smith, J.S. de Souza, Trinuclear species in vanadium(II) chemistry, *J. Chem. Soc. Chem. Commun.* 13 (1994) 2137–2138.
- [50] S.C. Davies, D.L. Hughes, G.J. Leigh, J.R. Sanders, J.S. De Souza, Mono-, di-, and tri-nuclear complexes of iron(II) with N,N,N',N'-tetramethylethylenediamine, *J. Chem. Soc. Dalton Trans.* (1997) 1981–1988.
- [51] D.A. Handley, P.B. Hitchcock, G.J. Leigh, Triangulo-pentahalotrimetal complexes of nickel (II) and cobalt (II) with N,N,N',N'-tetramethylethane-1,2-diamine and related compounds, *Inorganica Chim. Acta* 314 (2001) 1–13.
- [52] P. Sobota, J. Utko, S. Szafert, Z. Janas, T. Glowiaik, Polynuclear aggregation of cobalt and manganese dichlorides, *J. Chem. Soc. Dalton Trans.* (1996) 3469–3473.
- [53] J.C. Röder, F. Meyer, H. Pritzkow, An unusual hexanickel cage complex with u- and u₃-chloro bridges and an interstitial u₆-chloride, *Chem. Commun.* 2176–2177 (2001).
- [54] G. Noël, J.C. Röder, S. Dechert, H. Pritzkow, L. Bolk, S. Mecking, F. Meyer, Pyrazolate-based dinuclear a-diimine-type palladium(II) and nickel(II) complexes – a bimetallic approach in olefin polymerisation, *Adv. Synth. Catal.* 348 (2006) 887–897.
- [55] A. Ghisolfi, K.Y. Monakhov, R. Paccagnini, P. Braunstein, X. López, C. De Graaf, M. Speldrich, J. Van Leusen, H. Schilder, P. Kögerler, A comparative synthetic, magnetic and theoretical study of functional M4Cl₄ cubane-type Co(II) and Ni (II) complexes, *Dalton Trans.* 43 (2014) 7847–7859.
- [56] M. Xie, C. Han, J. Zhang, G. Xie, H. Xu, White electroluminescent phosphine-chelated copper iodide nanoclusters, *Chem. Mater.* 29 (2017) 6606–6610.
- [57] J. Rosales, J.M. Garcia, E. Ávila, T. González, D.S. Coll, E. Ocando-Mávarez, A novel tetramer copper (II) complex containing diallylphosphine ligands, *Inorganica Chim. Acta* 467 (2017) 155–162.
- [58] Q. Li, J.B. Vincent, E. Libby, H.-R. Chang, J.C. Huffman, P.D.W. Boyd, G. Christou, D.N. Hendrickson, Structure, magnetochemistry and biological relevance of [Mn₄O₃Cl₄(OAc)₃(py)]₃, a complex with S=9/2 ground state, *Angew. Chem. Int. Ed.* 27 (1988) 1731–1733.
- [59] M.W. Wemple, H. Tsai, K. Folting, D.N. Hendrickson, G. Christou, Distorted cubane [Mn₄O₃C₁]⁶⁺ complexes with arene-carboxylate ligation, *Inorg. Chem.* 32 (1993) 2025–2031.
- [60] U. Riese, N. Faza, W. Massa, K. Harms, T. Breyhan, P. Knochel, J. Ensling, V. Ksenofontov, P. Gülich, K. Dehnicke, Phosphoraneiminato complexes of manganese and cobalt with heterocubane structure, *Z. Anorg. Allg. Chem.* 625 (1999) 1494–1499.
- [61] J.S. Bashkin, H.-R. Chang, W.E. Streib, J.C. Huffman, D.N. Hendrickson, G. Christou, Modelling the photosynthetic water oxidation center, *J. Am. Chem. Soc.* 109 (1987) 6502–6504.
- [62] S. Wang, K. Folting, W.E. Streib, E.A. Schmitt, J.K. McCusker, D.N. Hendrickson, G. Christou, Chloride-induced conversion of [Mn₄O₂(OAc)₆(py)₂(dbm)₂] to [Mn₄O₃Cl(OAc)₃(dbm)₃], *Angew. Chem. Int. Ed.* 30 (1991) 305–306.
- [63] S. Wang, H.-L. Tsai, W.E. Streib, G. Christou, D.N. Hendrickson, Bromide incorporation into a high-oxidation-state manganese aggregate, and reversible redox processes for the [Mn₄O₃X(OAc)₃(dbm)₃] (X = Cl, Br) complexes, *J. Chem. Soc. Chem. Commun.* 1427–1429 (1992).
- [64] D.N. Hendrickson, J.G. Christou, E.A. Schmitt, E. Libby, J.S. Bashkin, S. Wang, H. Tsai, J.B. Vincent, P.D.W. Boyd, J.C. Huffman, K. Folting, Q. Li, W.E. Streib, Photosynthetic water oxidation center: spin frustration in distorted cubane Mn₄V₁Mn₁I₃ model complexes, *J. Am. Chem. Soc.* 114 (1992) 2455–2471.
- [65] S. Wang, H. Tsai, E. Libby, K. Folting, W.E. Streib, D.N. Hendrickson, G. Christou, Modeling the photosynthetic water oxidation center, *Inorg. Chem.* 35 (1996) 7578–7589.
- [66] M.W. Wemple, D.M. Adarm, K. Folting, D.N. Hendrickson, G. Christou, Incorporation of fluoride into a tetranuclear Mn/O/RCO₂ aggregate, *J. Am. Chem. Soc.* 117 (1995) 7275–7276.
- [67] S.P. Perleps, J.C. Huffman, G. Christou, Preparation and characterization of [Mn₁₁O₁₀Cl₂(OAc)₁₁(bpy)₂(MeCN)₂(H₂O)₂](ClO₄)₂*8MeCN, a Mixed-valence manganese(III/IV) aggregate with rare undecanuclearity, *J. Chem. Soc. Chem. Commun.* 23 (1991) 1657–1659.
- [68] M.M. Hänninen, J. Väliaara, J. Cano, R. Sillanpää, E. Colacio, Experimental and computational study of unique tetrานuclear μ₃-Chloride and μ-phenoxy/chloro-bridged defective dicubane cobalt (II) clusters, *Eur. J. Inorg. Chem.* 1192–1199 (2016).
- [69] G. Aromi, M.J. Knapp, J. Claude, J.C. Huffman, D.N. Hendrickson, G. Christou, High-spin molecules : hexanuclear mn₃i₃ clusters with [Mn₆O₄X₄]⁶⁺ face-capped octahedral cores and S = 12 ground states, *J. Am. Chem. Soc.* 121 (1999) 5489–5499.
- [70] M. Viciana-Chumillas, G. de Ruiter, S. Tanase, J.M.M. Smits, R. de Gelder, I. Mutikainen, U. Turpeinen, L.J. de Jongh, J. Reedijk, High nuclearity manganese (III) compounds containing phenol-pyrazole ligands: the influence of the ligand on the core geometry, *Dalton Trans.* 39 (2010) 4991–4998.
- [71] G. Aromi, J.-P. Claude, M.J. Knapp, J.C. Huffman, D.N. Hendrickson, G. Christou, High-spin molecules: hexanuclear [Mn₆O₄Cl₄(Me₂dbm)₆] with a near tetrahedral [Mn₆O₄Cl₄]⁶⁺ core and a S = 12 ground state, *J. Am. Chem. Soc.* 120 (1998) 2977–2978.
- [72] J. Utko, A.B. Canaj, C.J. Milios, M. Sobocińska, T. Lis, New members in the [Mn₁₀] supertetrahedron family, *Inorg. Chem. Commun.* 45 (2014) 71–74.
- [73] M. Manoli, A. Collins, S. Parsons, A. Candini, M. Evangelisti, E.K. Brechin, Mixed-valent Mn supertetrahedra and planar discs as enhanced magnetic coolers, *J. Am. Chem. Soc.* 130 (2008) 11129–11139.
- [74] D.P. Goldberg, A. Caneschi, S.J. Lippard, A decanuclear mixed-valent manganese complex with a high spin multiplicity in the ground state, *J. Am. Chem. Soc.* 115 (1993) 9299–9300.
- [75] S. Nayak, M. Evangelisti, A.K. Powell, J. Reedijk, Magnetothermal studies of a series of coordination clusters built from ferromagnetically coupled Mn₁₁4Mn₃I₆ supertetrahedral units, *Chem. - A Eur. J.* 16 (2010) 12865–12872.
- [76] S. Stuiber, G. Wu, J. Nehrkorn, J. Dreiser, Y. Lan, G. Novitchi, C.E. Anson, T. Unruh, A.K. Powell, O. Waldmann, Inelastic neutron scattering on an Mn₁₀ supertetrahedron: assessment of exchange coupling constants, ferromagnetic spin waves and an analogy to the Hückel method, *Chem. - A Eur. J.* 17 (2011) 9094–9106.
- [77] M. Manoli, R.D.L. Johnstone, S. Parsons, M. Murrie, M. Affronte, M. Evangelisti, E.K. Brechin, A ferromagnetic mixed-valent Mn supertetrahedron: towards low-temperature magnetic refrigeration with molecular clusters, *Angew. Chem. Int. Ed.* 46 (2007) 4456–4460.
- [78] D.P. Goldberg, A. Caneschi, C.D. Delfs, R. Sessoli, S.J. Lippard, A decanuclear manganese cluster with Oxo and halide bridging ligands, *J. Am. Chem. Soc.* 117 (1995) 5789–5800.
- [79] S.M. Taylor, R.D. McIntosh, J. Reze, S.J. Dalgarno, E.K. Brechin, Oxacalix[3] arene-supported supertetrahedron, *Chem. Commun.* 48 (2012) 9263–9265.
- [80] H. Wang, X. Song, H. Zhou, Y. Chen, Y. Xu, Y. Song, Synthesis, crystal structure and magnetic properties of an enneanuclear manganese cluster containing mixed chelating ligands, *Polyhedron* 30 (2011) 3206–3210.
- [81] A.M. Ako, I.J. Hewitt, V. Mereacre, R. Clérac, W. Wernsdorfer, C.E. Anson, A.K. Powell, A ferromagnetically coupled Mn₁₉ aggregate with a record S = 83/2 ground spin state, *Angew. Chem. Int. Ed.* 45 (2006) 4926–4929.
- [82] A.M. Ako, Y. Lan, O. Hampe, E. Cremades, E. Ruiz, C.E. Anson, A.K. Powell, All-round robustness of the Mn 19 coordination cluster system : experimental validation of a theoretical prediction, *Chem. Commun.* 50 (2014) 5847–5850.
- [83] E. Ruiz, T. Cauchy, J. Cano, R. Costa, J. Tercero, S. Alvarez, Magnetic structure of the large-spin Mn₁₀ and Mn₁₉ complexes: a theoretical complement to an experimental milestone, *J. Am. Chem. Soc.* 130 (2008) 7420–7426.
- [84] A.M. Ako, B. Burger, Y. Lan, V. Mereacre, R. Clérac, G. Butth, S. Gómez-Coca, E. Ruiz, C.E. Anson, A.K. Powell, Magnetic interactions mediated by diamagnetic cations in [Mn₁₈M] coordination clusters, *Inorg. Chem.* 52 (2013) 5764–5774.
- [85] A.M. Ako, V. Mereacre, R. Clérac, W. Wernsdorfer, I.J. Hewitt, C.E. Anson, A.K. Powell, A [Mn₁₈Dy] SMM resulting from the targeted replacement of the central Mn₁₁ in the S = 83/2 [Mn₁₉] aggregate with Dy^{III}, *Chem. Commun.* 544–546 (2009).
- [86] S. Mameri, A.M. Ako, F. Yesil, M. Hibert, Y. Lan, C.E. Anson, A.K. Powell, Coordination cluster analogues of the high-spin [Mn₁₉] system with functionalized 2,6-Bis(hydroxymethyl)phenol ligands, *Eur. J. Inorg. Chem.* 4326–4334 (2014).
- [87] C. Liu, R. Xiong, D. Zhang, D. Zhu, Nanoscale homochiral C₃-symmetric mixed-valence manganese cluster complexes with both ferromagnetic and ferroelectric properties, *J. Am. Chem. Soc.* 132 (2010) 4044–4045.
- [88] M. Charalambous, E.E. Moushi, C. Papariantafyllopoulou, W. Wernsdorfer, V. Nastopoulos, G. Christou, A.J. Tasiopoulos, A Mn₃₆Ni₄ “loop-of-loops-and-supertetrahedra” aggregate possessing a high S = 26 ± 1 spin ground state, *Chem. Commun.* 48 (2012) 5410–5412.
- [89] S. Nayak, L.M.C. Beltran, Y. Lan, R. Clérac, N.G.R. Hearns, W. Wernsdorfer, C.E. Anson, A.K. Powell, Two edge-sharing Mn₁₁4Mn₃I₆ supertetrahedra give an anisotropic S = 28 ± 1 Mn₁₁6Mn₃I₁₁ complex, *Dalton Trans.* 1901–1903 (2009).
- [90] D. Aravena, D. Venegas-Yazigi, E. Ruiz, Exchange interactions on the highest-spin reported molecule: the mixed-valence Fe 42 complex, *Sci. Rep.* 6 (2016) 23847.
- [91] M. Hirotsu, Y. Shimizu, N. Kuwamura, R. Tanaka, I. Kinoshita, R. Takada, Y. Teki, H. Hashimoto, Anion-controlled assembly of four manganese ions: structural, magnetic, and electrochemical properties of tetramanganese complexes stabilized by xanthene-bridged schiff base ligands, *Inorg. Chem.* 51 (2012) 766–768.
- [92] A. Sachse, S. Demeshko, F. Meyer, Structural and magnetic variability of cobalt (II) complexes with bridging pyrazolate ligands bearing appended imine groups, *Dalton Trans.* 7756–7764 (2009).
- [93] A. Sachse, S. Demeshko, S. Dechert, V. Daebel, A. Lange, F. Meyer, Highly preorganized pyrazolate-bridged palladium (II) and nickel (II) complexes in bimetallic norbornane polymerization, *Dalton Trans.* 39 (2010) 3903–3914.
- [94] O.M. Yaghi, M. O’Keefe, N.W. Ockwig, H.K. Chae, M. Eddaoudi, J. Kim, Reticular synthesis and the design of new materials, *Nature* 423 (2003) 705–714.
- [95] Z. Guo, D. Yan, H. Wang, D. Tesfagaber, X. Li, Y. Chen, W. Huang, B. Chen, A three-dimensional microporous metal-metallocloporphyrin framework, *Inorg. Chem.* 200–204 (2015).
- [96] D.J. Xiao, M.I. Gonzalez, L.E. Darago, K.D. Vogiatzis, E. Haldoupis, L. Gagliardi, J. R. Long, Selective, tunable O₂ binding in cobalt(II) – triazolate/pyrazolate metal-organic frameworks, *J. Am. Chem. Soc.* 138 (2016) 7161–7170.

- [97] D.A. Reed, D.J. Xiao, M.I. Gonzalez, L.E. Darago, Z.R. Herm, F. Grandjean, J.R. Long, Reversible CO scavenging via adsorbate-dependent spin state transitions in an iron(II) – Triazolate metal-organic framework, *J. Am. Chem. Soc.* 138 (2016) 5594–5602.
- [98] X. Wang, L. Zhang, J. Yang, F. Dai, R. Wang, D. Sun, Metal-ion metathesis and properties of triarylboron-functionalized metal-organic frameworks, *Chem. – An Asian J.* 10 (2015) 1535–1540.
- [99] K. Sumida, S. Horike, S.S. Kaye, Z.R. Herm, W.L. Queen, C.M. Brown, F. Grandjean, G.J. Long, A. Dailly, J.R. Long, Hydrogen storage and carbon dioxide capture in an iron-based sodalite-type metal – organic framework discovered via high-throughput methods, *Chem. Sci.* 1 (2010) 184–191.
- [100] F.-J. Ma, S.-X. Liu, C.-Y. Sun, D.-D. Liang, G.-J. Ren, F. Wei, Y.-G. Chen, Z.-M. Su, A sodalite-type porous metal-organic framework with polyoxometalate templates: adsorption and decomposition of dimethyl methylphosphonate, *J. Am. Chem. Soc.* 133 (2011) 4178–4181.
- [101] S.-D. Han, J.-P. Zhao, Y.-Q. Chen, S.-J. Liu, X.-H. Miao, T.-L. Hu, X.-H. Bu, A spin-canted polynuclear manganese complex comprised of alternating linkage of cyclic tetra- and mononuclear fragments, *Cryst. Growth Des.* 14 (2014) 2–5.
- [102] L. Xie, S. Liu, C. Gao, R. Cao, J. Cao, C. Sun, Z. Su, Mixed-valence iron (II, III) trimates with open frameworks modulated by solvents, *Inorg. Chem.* 46 (2007) 7782–7788.
- [103] G. Liu, B.-B. Li, Y.-X. Tan, K. Su, D. Yuan, Comparative stability and sorption study of two the-type metal-organic frameworks with different multiplicate metal-ligand interactions in secondary building units, *Cryst. Growth Des.* 17 (2017) 418–422.
- [104] Y. Kim, S. Das, S. Bhattacharya, S. Hong, M.G. Kim, M. Yoon, S. Natarajan, K. Kim, Metal-ion metathesis in metal-organic frameworks: a synthetic route to new metal-organic frameworks, *Chem. – A Eur. J.* 18 (2012) 16642–16648.
- [105] J.-H. Liao, W.-T. Chen, C.-S. Tsai, C.-C. Wang, Characterization, adsorption properties, metal ion-exchange and crystal-to-crystal transformation of Cd3 [(Cd4Cl)3(BTT)8(H2O)12]2 framework, *CrystEngComm.* 15 (2013) 3377–3384.
- [106] C.K. Brozek, A.F. Cozzolino, S.J. Teat, Y. Chen, M. Dincă, Quantification of Site-specific cation exchange in metal-organic frameworks using multi-wavelength anomalous X-ray dispersion, *Chem. Mater.* 25 (2013) 2998–3002.
- [107] I. Timokhin, A.J.P. White, P.D. Lickiss, C. Pettinari, R.P. Davies, Microporous metal-organic frameworks built from rigid tetrahedral tetrakis(4-tetrazolylphenyl)silane connectors, *CrystEngComm.* 16 (2014) 8094–8097.
- [108] M. Dincă, A. Dailly, Y. Liu, C.M. Brown, D.A. Neumann, J.R. Long, Hydrogen storage in a microporous metal-organic framework with exposed Mn²⁺ coordination sites, *J. Am. Chem. Soc.* 128 (2006) 16876–16883.
- [109] Q. Meng, J. Liu, X. Long, S. Zhang, Y. Quan, A porous the-type metal-organic framework based on [Mn4Cl]⁷⁺ clusters for selective gas sorption, *Inorg. Chem. Commun.* 79 (2017) 46–49.
- [110] M. Lamouchi, E. Jeanneau, A. Pillonnet, A. Brioude, M. Martini, O. Stéphan, F. Meganem, G. Novitchi, D. Luneau, C. Desroches, Tetranuclear manganese(II) complexes of sulfonylcalix[4]arene macrocycles: synthesis, structure, spectroscopic and magnetic properties, *Dalton Trans.* 41 (2012) 2707–2713.
- [111] Y. Suffren, N. O'Toole, A. Hauser, E. Jeanneau, A. Brioude, C. Desroches, Discrete polynuclear manganese(II) complexes with thiocalixarene ligands: synthesis, structures and photophysical properties, *Dalton Trans.* 44 (2015) 7991–8000.
- [112] H. Tan, S. Du, Y. Bi, W. Liao, Two 2D metal-calixarene aggregates incorporating pre-designed coordination nanocages, *Chem. Commun.* 49 (2013) 8211–8213.
- [113] S. Wang, Y. Bi, W. Liao, Constructing calixarene-supported high nuclearity Co₂₇, Co₂₈ and Ni₁₈Na₆ clusters with triazoles as co-bridges, *CrystEngComm.* 17 (2015) 2896–2902.
- [114] M. Liu, W. Liao, C. Hu, S. Du, H. Zhang, Calixarene-based nanoscale coordination cages, *Angew. Chem. Int. Ed.* 51 (2012) 1585–1588.
- [115] K. Su, F. Jiang, J. Qian, Y. Gai, M. Wu, S.M. Bawaked, M. Mokhtar, S.A. Al-Thabaiti, M. Hong, Generalized synthesis of calixarene-based high-nuclearity M₄n nanocages, *Cryst. Growth Des.* 14 (2014) 3116–3123.
- [116] M. Liu, W. Liao, Bridging calixarene-based Co₄ units into a square or belt with aromatic dicarboxylic acids, *CrystEngComm.* 14 (2012) 5727–5729.
- [117] M. Liu, S. Du, W. Liao, A metal–organic coordination nanotube based on Co₄-TC4A subunits and V-shaped aromatic dicarboxylic acids, *J. Mol. Struct.* 1049 (2013) 310–314.
- [118] W. Liu, M. Liu, S. Du, Y. Li, W. Liao, Bridging cobalt–calixarene subunits into a Co₈ entity or a chain with 4,4'-bipyridyl, *J. Mol. Struct.* 1060 (2014) 58–62.
- [119] K. Su, F. Jiang, J. Qian, J. Pang, F. Hu, S.M. Bawaked, M. Mokhtar, S.A. Al-Thabaiti, M. Hong, Bridging different Co₄-calix[4]arene building blocks into grids, cages and 2D polymers with chiral camphoric acid, *CrystEngComm.* 17 (2015) 1750–1753.
- [120] X. Hang, S. Wang, X. Zhu, H. Han, W. Liao, pH-dependent formation of different coordination cages based on Co₄-TC4A secondary building units and bridging ligands, *CrystEngComm.* 18 (2016) 4938–4943.
- [121] Y. Bi, S. Du, W. Liao, p-tert-Butylthiocalix[4]arene-supported high-nuclearity Co₂₄M₈ nanospheres and the hybrids with Keggin polyoxometalates, *Chem. Commun.* 47 (2011) 4724–4726.
- [122] Y. Bi, X.-T. Wang, W. Liao, X. Wang, X. Wang, H. Zhang, S. Gao, A Co₃₂ nanosphere supported by p-tert-butylthiocalix[4]arene, *J. Am. Chem. Soc.* 131 (2009) 11650–11651.
- [123] A. Bilyk, A.K. Hall, J.M. Harrowfield, W. Hosseini, G. Mislin, B.W. Skelton, C. Taylor, A.H. White, Linear, divergent molecular receptors – Subtle effects of transition metal coordination geometry, *Eur. J. Inorg. Chem.* 823–826 (2000).
- [124] A. Bilyk, J.W. Dunlop, R.O. Fuller, A.K. Hall, J.M. Harrowfield, M.W. Hosseini, G. A. Koutsantonis, I.W. Murray, B.W. Skelton, R.L. Stamps, A.H. White, Systematic structural coordination chemistry of p-tert-butyltetraethylthiocalix[4]arene: further complexes of transition-metal ions, *Eur. J. Inorg. Chem.* 2106–2126 (2010).
- [125] M. Wu, D. Yuan, L. Han, B. Wu, Y. Xu, M. Hong, Inclusion of metal complexes into cavities of 2D coordination networks built from p-sulfonatothiocalix[4]arene tetranuclear clusters, *Eur. J. Inorg. Chem.* 526–530 (2006).
- [126] F. Dai, Z. Wang, Modular assembly of metal – Organic supercontainers incorporating sulfonylcalixarenes, *J. Am. Chem. Soc.* 134 (2012) 8002–8005.
- [127] S. Du, C. Hu, J. Xiao, H. Tan, W. Liao, A giant coordination cage based on sulfonylcalix[4]arenes, *Chem. Commun.* 48 (2012) 9177–9179.
- [128] F.-R. Dai, Y. Qiao, Z. Wang, Designing structurally tunable and functionally versatile synthetic supercontainers, *Inorg. Chem. Front.* 3 (2016) 243–249.
- [129] S. Wang, X. Gao, X. Hang, X. Zhu, H. Han, W. Liao, W. Chen, Ultrafine Pt nanoclusters confined in a calixarene-based {Ni₂₄} coordination cage for high-efficient hydrogen evolution reaction, *J. Am. Chem. Soc.* 138 (2016) 16236–16239.
- [130] L. Zhang, R. Clérac, P. Heijboer, W. Schmitt, Influencing the symmetry of high-nuclearity and high-spin manganese oxo clusters: supramolecular approaches to manganese-based keplerates and chiral solids, *Angew. Chem. Int. Ed.* 51 (2012) 3007–3011.
- [131] L. Zhang, T. Chimamkpam, C.I. Onet, N. Zhu, R. Clérac, W. Schmitt, Anion-directed supramolecular chemistry modulating the magnetic properties of nanoscopic Mn coordination clusters: from polynuclear high-spin complexes to SMMs, *Dalton Trans.* 45 (2016) 17705–17713.
- [132] L. Zhang, R. Clérac, C.I. Onet, M. Venkatesan, P. Heijboer, W. Schmitt, Supramolecular approach by using Jahn – Teller sites to construct a [Mn₁₃]-based coordination polymer and modify its magnetic properties, *Chem. Eur. J.* 18 (2012) 13984–13988.
- [133] C. Streb, Structure and bonding in molecular vanadium oxides: from templates via host – Guest chemistry to applications, *Struct. Bond.* (2017) 1–17.
- [134] M. Rohmer, M. Bénard, J.-P. Blaudeau, J.-M. Maestre, J.M. Poblet, From Lindqvist and Keggin ions to electronically inverse hosts : Ab initio modelling of the structure and reactivity of polyoxometalates, *Coord. Chem. Rev.* 178–180 (1998) 1019–1049.
- [135] C. Healy, B. Twamley, M. Venkatesan, S. Schmidt, T. Gunnlaugsson, W. Schmitt, Hetero-metallic, functionalizable polyoxomolybdate clusters via a “top-down” synthetic method, *Chem. Commun.* 53 (2017) 10660–10663.
- [136] C.I. Onet, L. Zhang, R. Clérac, J.B. Jean-Denis, M. Feeney, T. McCabe, W. Schmitt, Self-assembly of hybrid organic – Inorganic polyoxomolybdates: solid-state structures and investigation of formation and core rearrangements in solution, *Inorg. Chem.* 50 (2011) 604–613.
- [137] M.-M. Rohmer, J. Devémry, R. Wiest, M. Bénard, Ab initio modeling of the endohedral reactivity of polyoxometallates, *J. Am. Chem. Soc.* 118 (1996) 13007–13014.
- [138] P. Song, W. Guan, L. Yan, C. Liu, C. Yao, Z. Su, Theoretical study on the tetranuclear endohedral vanadyl carboxylates with guest-switchable redox properties and large polarizability, *Dalton Trans.* 39 (2010) 3706–3713.
- [139] V.W. Day, W.G. Klemperer, O.M. Yaghi, Synthesis and characterization of a soluble oxide inclusion complex, *J. Am. Chem. Soc.* 111 (1989) 5959–5961.
- [140] W.G. Klemperer, T.A. Marquart, O.M. Yaghi, New directions in polyvanadate chemistry: from cages and clusters to baskets, belts, bowls, and barrels, *Angew. Chem. Int. Ed.* 31 (1992) 49–51.
- [141] D. Sahoo, R. Suriyanarayanan, V. Chandrasekhar, Di-, tri- and tetranuclear molecular vanadium phosphonates: a chloride encapsulated tetranuclear bowl, *Dalton Trans.* 43 (2014) 10898–10909.
- [142] J. Salta, J. Zubietia, Solvothermal synthesis and crystal structure of (Ph₄P)₄[(VO₂)₄(CH₃CO₂)₄Cl], *Inorganica Chem. Acta* 252 (1996) 435–438.
- [143] S. Konar, A. Clearfield, Mixed-valent dodecanuclear vanadium cluster encapsulating chloride anions and its reaction to form a “Bowl”-shaped cluster, *Inorg. Chem.* 47 (2008) 3492–3494.
- [144] J.M. Breen, W. Schmitt, Hybrid organic-inorganic polyoxometalates: Functionalization of V₁₉/V₂₀ nanosized clusters to produce molecular capsules, *Angew. Chem. Int. Ed.* 47 (2008) 6904–6908.
- [145] J.M. Breen, R. Clérac, L. Zhang, S.M. Cloonan, E. Kennedy, M. Feeney, T. McCabe, C.D. Williams, W. Schmitt, Self-assembly of hybrid organic-inorganic polyoxovanadates: functionalised mixed-valent clusters and molecular cages, *Dalton Trans.* 41 (2012) 2918–2926.
- [146] J.M. Breen, L. Zhang, R. Clement, W. Schmitt, Hybrid polyoxovanadates: anion-influenced formation of nanoscopic cages and supramolecular assemblies of asymmetric clusters, *Inorg. Chem.* 51 (2012) 19–21.
- [147] L. Zhang, W. Schmitt, From platonic templates to archimedean solids: successive construction of nanoscopic V₁₆As₈, {V₁₆As₁₀}, {V₂₀As₈}, and {V₂₄As₈} polyoxovanadate cages, *J. Am. Chem. Soc.* 133 (2011) 11240–11248.
- [148] Z. Zhang, L. Wojtas, M.J. Zaworotko, Organic – inorganic hybrid polyhedra that can serve as supermolecular building blocks, *Chem. Sci.* 5 (2014) 927–931.
- [149] Z. Zhang, W. Gao, L. Wojtas, Z. Zhang, M.J. Zaworotko, A new family of anionic organic-inorganic hybrid doughnut-like nanostructures, *Chem. Commun.* 51 (2015) 9223–9226.

- [150] G.B. Karet, Z. Sun, D.D. Heinrich, J.K. McCusker, K. Folting, W.E. Streib, J.C. Huffman, D.N. Hendrickson, G. Christou, Tetranuclear and pentanuclear vanadium (IV/V) carboxylate complexes, *Inorg. Chem.* 35 (1996) 6450–6460.
- [151] D.D. Heinrich, K. Folting, W.E. Streib, J.C. Huffman, G. Christou, Synthesis of tetranuclear and pentanuclear vanadium-oxide-carboxylate aggregates, *J. Chem. Soc. Chem. Commun.* 1411–1413 (1989).
- [152] Y. Zhang, X. Wang, S. Li, B. Song, K. Shao, Z. Su, Ligand-directed assembly of polyoxovanadate-based metal-organic polyhedra, *Inorg. Chem.* 55 (2016) 8770–8775.
- [153] M.B. Mahimaidoss, S.A. Krasnikov, L. Reck, C.I. Onet, J.M. Breen, N. Zhu, B. Marzec, I.V. Shvets, W. Schmitt, Homologous size-extension of hybrid vanadate capsules – solid state structures, solution stability and surface deposition, *Chem. Commun.* 50 (2014) 2265–2267.
- [154] L. Zhang, B. Marzec, R. Clérac, Y. Chen, H. Zhang, W. Schmitt, Supramolecular approaches to metal-organic gels using “Chevrel-type” coordination clusters as building units, *Chem. Commun.* 49 (2013) 66–68.
- [155] J. Liu, C. Ma, H. Chen, C. Chen, Synthesis, crystal structures and magnetic properties of a family of manganese phosphonate clusters with diverse structures, *CrystEngComm.* 17 (2015) 8736–8745.
- [156] J. Salta, Q. Chen, Y.-D. Chang, J. Zubieto, The oxovanadium – organophosphonate system, *Angew. Chem. Int. Ed.* 33 (1994) 757.
- [157] D. Wulff-Molder, M. Meisel, Synthesis and structural studies on molecular oxovanadium phosphonates, *Z. Anorg. Allg. Chem.* 634 (2008) 2966–2972.
- [158] M.I. Khan, Q. Chen, H. Höpe, S. Parkin, C.J. O’Connor, J. Zubieto, Hydrothermal synthesis and characterization of hexavanadium polyoxo alkoxide anion clusters, *Inorg. Chem.* 32 (1993) 2929–2937.
- [159] M.A. Kiskin, G.G. Aleksandrov, V.N. Ikorskii, V.M. Novotortsev, I.L. Eremenko, First hexanuclear manganese (II) μ_6 -Cl centered carboxylate anion: Synthesis, structure and magnetic properties, *Inorg. Chem. Commun.* 10 (2007) 997–1000.
- [160] Y.-L. Miao, J.-L. Liu, Z.-J. Lin, Y.-C. Ou, J.-D. Leng, M.-L. Tong, Synthesis, structures, adsorption behaviour and magnetic properties of a new family of polynuclear iron clusters, *Dalton Trans.* 39 (2010) 4893–4902.
- [161] Q. Chen, M.-H. Zeng, L.-Q. Wei, M. Kurmoo, A multifaceted cage cluster, $[\text{Co}6\text{O}12\text{X}]$: halide template effect and frustrated magnetism, *Chem. Mater.* 22 (2010) 4328–4334.
- [162] Y.-L. Miao, S.-D. Li, J.-L. Liu, F.-S. Guo, M.-L. Tong, Synthesis, structures and magnetic properties of octahedral clusters, *Inorg. Chem. Commun.* 52 (2015) 77–79.
- [163] V.A. Igonin, O.I. Shchegolikhina, S.V. Lindeman, M.M. Levitsky, Y.T. Struchkov, A.A. Zhdanov, Novel class of transition metal coordination compounds with macrocyclic organosiloxanolate ligands; their synthesis and crystal structure, *J. Organomet. Chem.* 423 (1992) 351–360.
- [164] G. Gavioli, R. Battistuzzi, P. Santi, C. Zucchi, G. Pályi, R. Ugo, A. Vizi-Orosz, O.I. Shchegolikhina, Y.A. Pozdniakova, S.V. Lindeman, A.A. Zhdanov, Bimetallic siloxane cluster of higher valent transition metals, *J. Organomet. Chem.* 485 (1995) 257–266.
- [165] C. Zucchi, M. Mattioli, A. Cornia, A.C. Fabretti, G. Gavioli, M. Pizzotti, R. Ugo, Y. A. Pozdniakova, O.I. Shchegolikhina, A.A. Zhdanov, G. Pályi, Bimetallic cyclosiloxanolate complexes of copper and nickel, *Inorganica Chim. Acta* 280 (1998) 282–287.
- [166] A. Cornia, A.C. Fabretti, G. Gavioli, C. Zucchi, M. Pizzotti, A. Vizi-Orosz, O.I. Shchegolikhina, Y.A. Pozdniakova, G. Pályi, Heterobimetallic cyclosiloxanolate sandwich clusters, *J. Clust. Sci.* 9 (1998) 295–318.
- [167] E.V. Govor, A.B. Lysenko, D. Quiñonero, E.B. Rusanov, A.N. Chernega, J. Moellmer, R. Staudt, H. Krautscheid, A. Frontera, K.V. Domasevitch, Self-assembly hexanuclear metallacontainer hosting halogenated guest species and sustaining structure of 3D coordination framework, *Chem. Commun.* 47 (2011) 1764–1766.
- [168] A. Müller, H. Reuter, S. Dillinger, Supramolecular inorganic chemistry: small guests in small and large hosts, *Angew. Chem. Int. Ed.* 34 (1995) 2328–2361.
- [169] K.Y. Monakhov, O. Linnenberg, P. Kozłowski, J. van Leusen, C. Besson, T. Secker, A. Ellern, X. López, J.M. Poblet, P. Kögerler, Supramolecular recognition influences magnetism in $[\text{X}@\text{HIV8V14054}]_6$ -self-assemblies with symmetry-breaking guest anions, *Chem. – A Eur. J.* 21 (2015) 2387–2397.
- [170] C.J. Calzado, J.M. Clemente-Juan, E. Coronado, A. Gaita-Arino, N. Suau, Role of the electron transfer and magnetic exchange interactions in the magnetic properties of mixed-valence polyoxovanadate complexes, *Inorg. Chem.* 47 (2008) 5889–5901.
- [171] K. Kastner, J.T. Margraf, T. Clark, C. Streb, A molecular placeholder strategy to access a family of transition-metal-functionalized vanadium oxide clusters, *Chem. – A Eur. J.* 20 (2014) 12269–12273.
- [172] Y. Inoue, Y. Kikukawa, S. Kuwajima, Y. Hayashi, A chloride capturing system via proton-induced structure transformation between opened- and closed-forms of dodecavanadates, *Dalton Trans.* 45 (2016) 7563–7569.
- [173] T. Kobayashi, S. Kuwajima, T. Kurata, Y. Hayashi, Structural conversion from bowl- to ball-type polyoxovanadates: synthesis of a spherical tetradevanadate through a chloride-incorporated bowl-type dodecavanadate, *Inorganica Chim. Acta* 420 (2014) 69–74.
- [174] K. Okaya, T. Kobayashi, Y. Koyama, Y. Hayashi, K. Isobe, Formation of VV lacunary polyoxovanadates and interconversion reactions of dodecavanadate species, *Eur. J. Inorg. Chem.* 5156–5163 (2009).
- [175] N. Kawanami, T. Ozeki, A. Yagasaki, NO-anion trapped in a molecular oxide bowl, *J. Am. Chem. Soc.* 122 (2000) 1239–1240.
- [176] K. Taisei, H. Yoshihito, I. Kiyoishi, Synthesis and characterisation of chloride-incorporated dodecavanadate from dicopper complex of macrocyclic octadevanadate, *Chem. Lett.* 39 (2010) 708–709.
- [177] K. Kastner, J. Forster, H. Ida, G.N. Newton, H. Oshio, C. Streb, Controlled reactivity tuning of metal-functionalized vanadium oxide clusters, *Chem. Eur. J.* 21 (2015) 7686–7689.
- [178] M. Šimuneková, D. Prodius, V. Mereacre, P. Schwendt, C. Turta, M. Bettinelli, A. Speghini, Y. Lan, C.E. Anson, A.K. Powell, Tetradecanuclear lanthanide-vanadium “nanochocolates”: catalytically-active cationic heteropolyoxovanadum clusters, *RSC Adv.* 3 (2013) 6299–6304.
- [179] J.M. Cameron, G.N. Newton, P. Busche, D.-L. Long, H. Oshio, L. Cronin, Synthesis and characterisation of a lanthanide-capped dodecavanadate cage, *Chem. Commun.* 49 (2013) 3395–3397.
- [180] J. Tucher, K. Peuntinger, J.T. Margraf, T. Clark, D.M. Guldi, C. Streb, Template-dependent photochemical reactivity of molecular metal oxides, *Chem. – A Eur. J.* 21 (2015) 8716–8719.
- [181] C. Streb, New trends in polyoxometalate photoredox chemistry : From photosensitisation to water oxidation catalysis, *Dalton Trans.* 41 (2012) 1651–1659.
- [182] A. Seliverstov, C. Streb, Chirality meets visible-light photocatalysis in a molecular cerium vanadium oxide cluster, *Chem. Commun.* 50 (2014) 1827–1829.
- [183] L. Chen, F. Jiang, Z. Lin, Y. Zhou, C. Yue, M. Hong, A basket tetradevanadate cluster with blue luminescence, *J. Am. Chem. Soc.* 127 (2005) 8588–8589.
- [184] A. Müller, E. Krückemeyer, M. Penk, H.-J. Walberg, H. Böggel, Spherical mixed-valence $[\text{V}15\text{O}36]^{5-}$, an example from an unusual cluster family, *Angew. Chem. Int. Ed.* 26 (1987) 1045–1046.
- [185] Y.-G. Li, Y. Lu, G.-Y. Luan, E.-B. Wang, Y. Duan, C.-W. Hu, N.-H. Hu, H.-Q. Jia, Hydrothermal syntheses and crystal structures of new cage-like mixed-valent polyoxovanadates, *Polyhedron* 21 (2002) 2601–2608.
- [186] H.N. Miras, R.G. Raptis, N. Lalioti, M.P. Sigalas, P. Baran, T.A. Kabanos, A novel series of vanadium-sulfite polyoxometalates: synthesis, structural, and physical studies, *Chem. – A Eur. J.* 11 (2005) 2295–2306.
- [187] Z. Yi, X. Yu, W. Xia, L. Zhao, C. Yang, Q. Chen, X. Wang, X. Xu, X. Zhang, Influence of the steric hindrance of organic amines on the supramolecular network based on polyoxovanadates, *CrystEngComm.* 12 (2010) 242–249.
- [188] H.-Y. Guo, T.-T. Zhang, P.-H. Lin, X. Zhang, X.-B. Cui, Q.-S. Huo, J.-Q. Xu, Preparation, structure and characterization of a series of vanadates, *CrystEngComm.* 19 (2017) 265–275.
- [189] C.-D. Zhang, S.-X. Liu, B. Gao, C.-Y. Sun, L.-H. Xie, M. Yu, J. Peng, Hybrid materials based on metal – organic coordination complexes and cage-like polyoxovanadate clusters: synthesis, characterization and magnetic properties, *Polyhedron*. 26 (2007) 1514–1522.
- [190] B. Dong, J. Peng, Y. Chen, Y. Kong, A. Tian, H. Liu, J. Sha, pH-controlled assembly of two polyoxovanadates based on $[\text{V}16\text{O}38\text{Cl}]^{8-}$ and $[\text{V}15\text{O}36\text{Cl}]^{6-}$ building blocks, *J. Mol. Struct.* 788 (2006) 200–205.
- [191] C.-L. Pan, J.-Q. Xu, G.-H. Li, D.-Q. Chu, T.-G. Wang, A three-dimensional framework of novel vanadium clusters bridged by $[\text{Ni}(\text{en})_2]^{2+}$, *Chem. – A Eur. J.* (2003) 1514–1517.
- [192] B.-X. Dong, J. Peng, C.J. Gomez-Garcia, S. Benmansour, H.-Q. Jia, N.-H. Hu, High-dimensional assembly depending on polyoxoanion templates, metal ion coordination geometries, and a flexible bis(imidazole) ligand, *Inorg. Chem.* 46 (2007) 5933–5941.